THE NICKEL-TITANIUM-CARBON SYSTEM

by

Edward Roy Stover

S.B., Massachusetts Institute of Technology, 1950

S.M., Massachusetts Institute of Technology, 1952

Submitted in Partial Fulfillment of the

Requirements for the Degree of

DOCTOR OF SCIENCE

at the

Massachusetts Institute of Technology

1956

Signature of Author
Department of Metallurgy
January 9, 1956

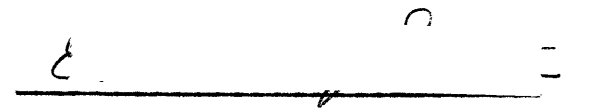

Signature of Professor
in Charge of Research

Signature of Chairman,
Departmental Committee
on Graduate Students.

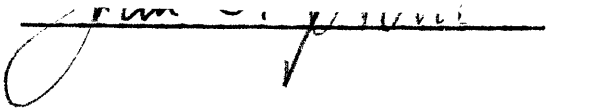

THE NICKEL-TITANIUM-CARBON SYSTEM

by

EDWARD ROY STOVER

Submitted to the Department of Metallurgy on January 9, 1956 in partial fulfillment of the requirements for the degree of Doctor of Science.

ABSTRACT

The system nickel-titanium-carbon has been studied on samples arc cast in helium, using metallographic, magnetic, X-ray and microhardness measurements. A tentative isothermal section at 870°C is presented, and the ternary solidus equilibria are reported. The solidus between titanium carbide and the nickel solid solution, and the precipitation of titanium carbide and graphite from the nickel solid solution are described in detail. The grain structures encountered in the cast alloys, and some of the effects of oxygen contamination are also illustrated.

It was found that titanium carbide forms two-phase fields with each of the nickel-titanium binary phases. The eta-2 structure, Ti_2Ni, dissolves at 870°C about 3 atomic per cent carbon, which increases the lattice parameter and microhardness. TiNi and $TiNi_3$ dissolve very little carbon. Nickel dissolves in titanium carbide to a very limited extent, but it causes a measurable lattice expansion.

The atomic per cent solubility in nickel of titanium carbide, together with graphite, was determined from the Curie points in the nickel solid solution as follows: 3.4 titanium plus 2.6 carbon at 1260°C, 3.1 titanium plus 1.2 carbon at 1000°C, and less than 2.0 titanium plus 0.2 carbon at 600°C. Graphite will precipitate from the binder of a pure ternary cermet at 1000°C or below, unless the binder contains 2 atomic per cent more titanium than carbon in solution.

Solidus temperatures in the vicinity of Ti_2Ni are increased by additions of carbon, and $Ti_2Ni(C)$ forms by a peritectic reaction between liquid and titanium carbide. The solidus in the vicinity of nickel, however, is lowered; a quasi-binary eutectic occurs at about 13 atomic per cent titanium and 4 atomic per cent carbon (at 1307°C). Two ternary eutectics, which produce a nickel solid solution, titanium carbide, and either graphite (at 1270°C), or $TiNi_3$ (at 1295°C) also occur. The plane between nickel and titanium carbide cuts through three-phase fields containing liquid or graphite.

Thesis Supervisor: John Wulff

Title: Professor of Metallurgy

TABLE OF CONTENTS

LIST OF ILLUSTRATIONS

Page

LIST OF TABLES

INTRODUCTION

During the past decade, titanium carbide cermets containing nickel and cobalt alloy binders have been widely studied for high temperature applications. With certain additions, such as molybdenum and chromium, the materials possess excellent creep strength and acceptable oxidation resistance. However, the impact strengths have been too low for many uses, even in the compositions containing high percentages of ductile binder.

It was believed that the production of cermets having superior mechanical properties might be aided by a better understanding of the phase composition changes taking place during sintering or infiltration, and during subsequent heating in service. Although the effects of the additives and impurities in commercial alloys are important, it was necessary to consider first the pure ternary, nickel - titanium - carbon. Since the nickel solid solution is the continuous phase in those compositions containing the highest strengths, principal emphasis was placed on the nickel corner of the system.

PREVIOUS WORK

Although many papers have been published on the structures and properties of titanium carbide - nickel cermets of different compositions (1), little quantitative data on the ternary solubility relationships have been reported. Zarubin and Molkov (2) first studied these alloys metallographically, and reported practically no solubility at either end of the quasi-binary, Ni - TiC. Edwards and Raine (3) examined several vacuum melted powder mixtures, after annealing for 24 hours at 1250°C, and reported that nickel dissolved between 3 and 5 weight per cent carbide. Some of the data presented here has been reported previously (4).

THE BINARY SYSTEMS

The information available on the three binary systems is summarized in Figure 1. The terms alpha and beta refer to the allotropic forms of titanium. The nickel solid solution is termed gamma, and the titanium carbide solid solution is termed delta.

The nickel-carbon binary is based principally on the summary by Hanson (5) of early thermal analysis and liquid solubility measurements. However, recent thermal analysis studies by Morrogh and Williams (6) show that, in the absence of supercooling, the eutectic temperature is around 1328°C, 10 to 15 degrees above that previously reported, and solidus measurements made during the work presented here confirmed this temperature within ± 3°C. The recent solid solubility measurements by Lander, Kern, and Beach (7) agree closely with the data shown by Kihlgren and Eash (8).

The nickel-titanium binary in Figure 1 is that obtained by Poole and Hume-Rothery (9). The previous determination by Margolin, Ence, and Nielsen (10) is essentially the same, except for the positions of the solidus and liquidus curves, particularly in the central portion of the diagram. The presence of carbon contamination in the earlier work might account for some of the differences, since melting determinations were made by annealing the samples in graphite crucibles.

The eutectoid decomposition of the disordered, body

Figure 1 - Binary systems carbon-nickel, nickel-titanium, and titanium-carbon, from data in the literature.

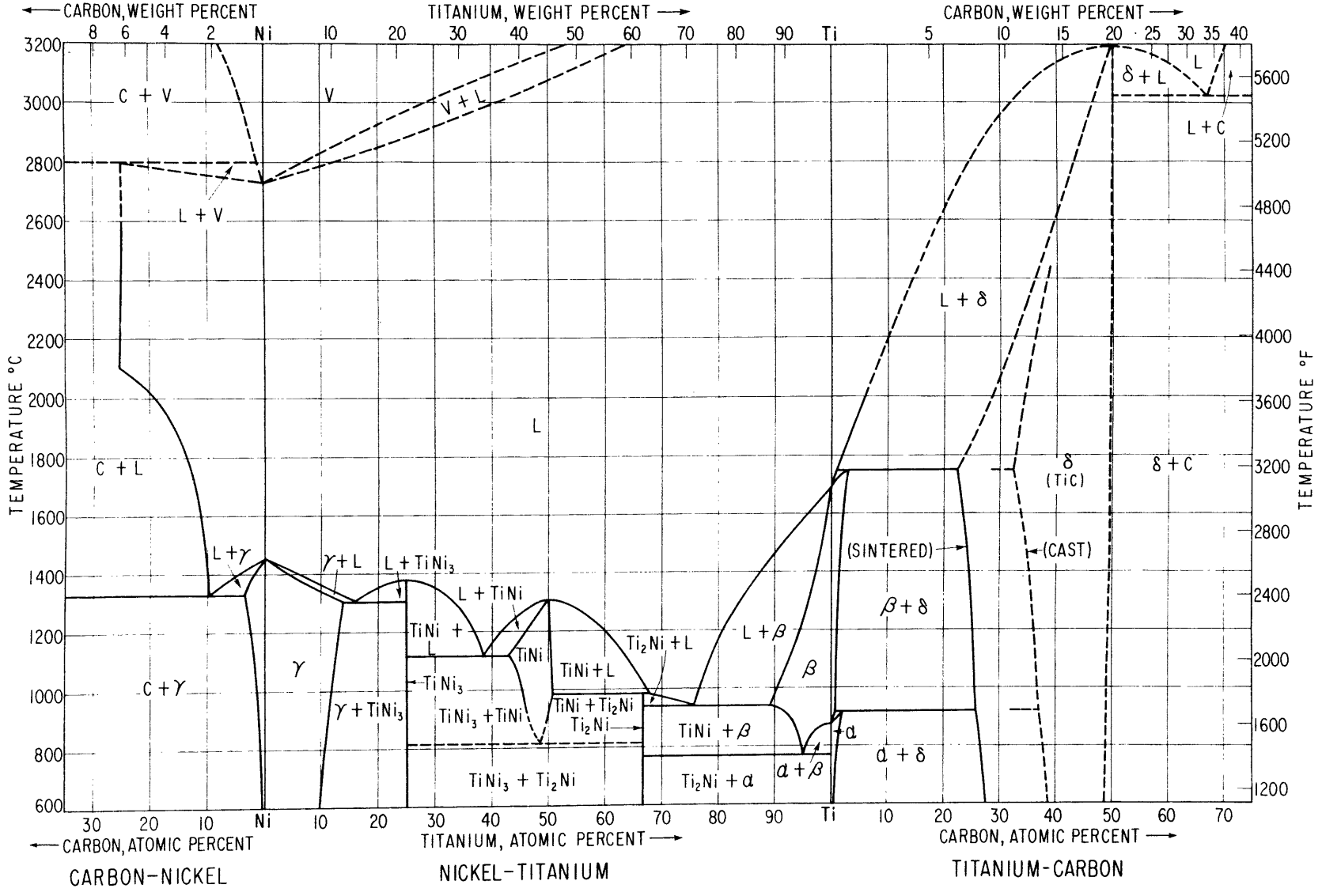
CARBON, WEIGHT PERCENT
TITANIUM, WEIGHT PERCENT
CARBON, WEIGHT PERCENT
TEMPERATURE °C
TEMPERATURE °F
C + V
V
V + L
L + V
C + L
L
L + γ
γ + L
L + TiNi3
L + TiNi
TiNi +
L
TiNi
TiNi + L
Ti2Ni + L
L + β
C + γ
γ
γ + TiNi3
TiNi3
TiNi3 + TiNi
TiNi + Ti2Ni
Ti2Ni
TiNi + β
β
α
α + β
α + δ
TiNi3 + Ti2Ni
Ti2Ni + α
L + δ
δ + L
L
L + C
δ
(TiC)
δ + C
(SINTERED)
(CAST)
β + δ
CARBON, ATOMIC PERCENT
TITANIUM, ATOMIC PERCENT
CARBON, ATOMIC PERCENT
CARBON-NICKEL
NICKEL-TITANIUM
TITANIUM-CARBON

centered cubic TiNi was first suggested by Duwez and Taylor (11) on the basis of powder mixtures annealed at 800°C and 650°C. Margolin, Ence, and Nielsen did not observe the reaction, but Hume-Rothery and Poole tend to confirm such a decomposition after long anneals at 600°C. The true equilibria in this region may be difficult to determine, since Rostoker (12) has shown that the presence of oxygen produces a $TiNi_3$ - $Ti_2Ni(O)$ two-phase field.

The titanium-carbon binary in Figure 1 is similar to that shown by McMullin and Norton (13). The titanium-rich region is the only accurate portion, and was determined by Cadoff and Nielsen (14) on arc melted alloys of high purity.

The solubility of titanium in the carbide, as determined on arc melted alloys by Cadoff and Nielsen is shown in the dotted line; the solubility presented by McMullin and Norton is shown as the solid line, which is based on powder mixtures which were sintered at pressures below one micron. In the present work, it was not possible to confirm which of the lines is closest to the true binary solubility, since homogenous alloys in thie region could not be prepared by the arc casting methods used.

The true solubility of carbon in titanium carbide is also in doubt, since oxygen and nitrogen contamination in commercial carbides reduces the carbon solubility, and data by Meerson and Krein (15) indicate that the carbon solubility changes with pressure.

The melting point maximum of titanium carbide has been reported from 3140 ± 90°C (16) to 3250°C (17); the temperature of the carbide - graphite eutectic appears to be at least 3000°C, since carbide powder has been hot pressed in graphite up to that temperature (18). The composition of the eutectic was estimated from arc cast structures encountered in the present work.

EXPERIMENTAL PROCEDURE

Alloy Preparation

Preliminary experiments made by melting powder mixtures in the vacua or inert atmospheres available usually showed modifications in the microstructures due to oxygen or nitrogen contamination. To minimize such contamination, all alloys were prepared by arc casting pure materials in purified helium.

The analyses of the starting materials are shown in Table I. The iodide titanium, contributed by the Foote Mineral Company, was used in certain Ti-C alloys, and in some compositions in the vicinity of the Ni-Ti binary; sponge titanium, produced by du Pont, was used in the rest. The vacuum melted nickel "A" was used in the alloys close to the Ni-Ti binary, and nickel "B" was used only in alloys containing more than 92 atomic per cent nickel. Nickel "C", contributed by the International Nickel Company, was used in alloys containing 50 to 95 per cent nickel. The carbon used was in the form of chips broken from spectroscopic graphite electrodes. Titanium carbide produced by Kennametal was also used in a few cases for comparison.

Ingots weighing between five and forty grams were arc-cast on a nickel-plated water-cooled copper crucible in a closed helium atmosphere. Spectroscopic graphite electrodes were used, except for a few nickel-titanium binary alloys, for which tungsten was used. Hot water was run beneath the

TABLE I: ANALYSIS OF STARTING MATERIALS

	Nickel A	Nickel B	Nickel C	Titanium (Iodide)*	Titanium (Sponge)	Carbon Rods	TiC** Kennametal
C	0.003	0.003	0.014	<0.001	--	(99.99)	19.66 total 0.60 free
O	0.0038	0.0015	--	0.002	--	--	--
N	0.00011	0.0006	--	0.002	0.015	--	--
B	--	--	<VST	--	--	--	--
Cl	--	--	--	--	0.085	--	--
Ca	--	--	<VST	0.0005	--	--	<0.01
Mg	<0.01	--	VST	0.0002	0.00	VST	<0.01
Al	--	--	VST	0.0001	0.02	--	<0.01
Si	0.0075	<0.0045	0.003	0.005	0.02	--	<0.01
Ti	Nil	--	--	--	--	--	79.22
V	--	--	--	--	--	--	1.0-0.01
Cr	--	--	--	0.0005	--	--	1.0-0.01
Mn	Nil	--	--	0.001	--	--	0.01
Fe	0.020	--	VST	0.0003	0.035	VST	1.0-0.01
Co	0.10	0.0050	ST	--	--	--	--
Ni	--	--	99.96	0.0001	--	--	<0.01
Cu	<0.01	--	VST	0.001	--	VST	<0.01

--: not determined.

ST: slight trace, spectroscopic analysis.

VST: very slight trace.

*: iodide titanium analysis typical of similar lots.

**: also less than 0.01 per cent Zn, W, Sn, Sb, Rb, P, Ag, by spectroscopic analysis.

crucible while the chamber was evacuated to about 15 microns, before the atmosphere was admitted. The helium was purified by passing it over titanium chips at about 800°C and activated charcoal at -178°C. The gas was held in a reservoir under a few centimeters positive pressure, so that it could be let into the chamber within a few seconds to minimize leakage, and the chamber was flushed twice with tank helium before the purified gas was admitted. Before the alloys were melted, several pieces of titanium sponge were always melted to further purify the gas. The ingots were turned over and remelted twice. They were then cut in two and examined metallographically for homogeneity. Chips for chemical analysis were machined from the sectioned surface of one half of each ingot analyzed.

Heat Treatment Procedure

To obtain an 870°C isothermal section, portions of the ingots were placed in a sealed, evacuated Vycor tube, along with some titanium sponge to serve as a getter. The tube was held in a chromel wound furnace for 100 hours before water quenching. The samples were then sectioned; one half was examined metallographically, and the other half was crushed into powder for X-ray analysis.

Solidus measurements in the nickel-rich region were made by heating wedges, cut from the ingots, in purified helium, which was gettered by titanium sponge, placed in the furnace near the samples. Boats of zirconia, which had

been pretreated by heating in hydrogen at 1000°C, were used to hold the samples. A zircon tube, heated by Glowbars, constituted the furnace chamber. The temperature directly above the samples was measured by a platinum - 10 per cent rhodium thermocouple, which was protected by a glazed porcelain sheath. The thermocouple was calibrated against the melting point of gold and the freezing point of copper, and the temperatures of the samples were checked with those measured when pieces of pure nickel or electrical copper were melted in the same positions.

To determine the solidus, the samples were held at different temperatures for 20 to 60 minutes and quenched into water. Such times were sufficient to cause solution and coalescence of the as-cast carbide eutectic structure at temperatures near the solidus, and the quench transformed any liquid present into an easily identified eutectic structure. Temperature measurement and control were accurate to within ± 3°C, and the tests for important compositions were repeated.

The procedure for the titanium rich samples was similar, except that nickel or molybdenum boats, a titanium-gettered argon atmosphere, and chromel-alumel thermocouples were used. In most cases, the rapid solidification of the liquid in these alloys also produced structures easily distinguishable from the solid phases.

The precipitation of titanium carbide and graphite from

the nickel solid solution was studied first by annealing samples out from the alloys used in the solidus determinations, and examining the microstructure and approximate Curie points. Curie points were estimated by determining the temperature of a liquid bath in which the samples were no longer attracted to an alnico magnet. Anneals for 24 hours at 1240°C, and 10 hours at 1200°C provided preliminary data, and showed that the maximum carbon solubility decreased more rapidly than the titanium solubility immediately below the solidus.

On the basis of these results, compositions were selected in the vicinity of the temperature versus composition trace of the nickel corner of the gamma + delta + carbon three-phase field. The positions of the solvus at different temperatures were studied primarily with samples located in the gamma + carbon field, where the tie lines were known exactly, and where equilibrium could be obtained in a relatively short time. The precipitation of carbide in these samples indicated the positions of the ternary corner of this gamma - carbon solvus at different temperatures, and these positions in turn located the gamma - delta solvus in the immediate vicinity. Compositions in the gamma + delta region were also studied, although it was expected that equilibrium would not be achieved as rapidly in these samples.

The ingot halves were pressed into rectangular blocks,

and annealed at 1260°C for one hour before quenching. Although the helium atmosphere was purified, and then gettered with titanium sponge in the vicinity of the samples, the atmosphere was not sufficiently pure to prevent surface oxidation of the higher titanium compositions. The scale was pickled off after the anneal, but its presence during the anneal prevented the use of a long homogenization treatment. However, the time used was sufficient to change the gamma + delta cast structure into an equilibrium gamma or gamma + carbon structure, and later examination showed that the carbon had diffused throughout the alloys.

The blocks were then swaged in nickel sheet to 1/8 inch rods, with several intermediate anneals of one to five minutes at 1260°C. After the final swaging (made without a sheath), part of each rod was annealed at 700°C for 370 hours in an evacuated Vycor bulb, and water quenched. Another part of each rod was annealed at 1260°C for one-half hour in a vacuum of 0.15 micron, and then cooled rapidly in a stream of helium in a cold portion of the vacuum system. The other portions of each rod were rolled flat, and cut into chips for determination of titanium and carbon.

The heat treated rods were then cut into cylinders about 1/8 inch long, and two cylinders of each composition, one annealed at 700°C, and one annealed at 1260°C, were annealed at each intermediate temperature. These samples were

continuously evacuated, at 0.10 micron or better, in a quartz or Vycor bulb suspended in a vertical furnace. After a time believed to be sufficient for achieving equilibrium, the Vycor connection to the vacuum system was melted or broken in two, and the bulb was allowed to drop into a solution of iced brine, where it was broken immediately. The samples were then weighed, and the Curie points were determined by the method described below. If samples cut from the same alloy had the same Curie points, it was assumed that equilibrium had been achieved at that temperature. Otherwise, the samples were swaged, squeezed to their original dimensions in a die, and then reannealed for a longer time. The final times of anneal are shown in Table II. The annealing times at 700°C and 600°C were not sufficient to

Table II: Annealing Times of Solvus Compositions

Temperature, °C	Time, hours
1265	1
1200	20
1100	49
1000	85
900	98
800	355
700	400
600	500

obtain equilibrium with respect to titanium carbide in all of the compositions.

Since there was some variation in titanium content between samples having the higher titanium compositions, the data were checked by reannealing the same specimens at

at several different temperatures, and by comparison with samples machined directly from the annealed ingots of some solid solution compositions. After all of the data had been taken on these specimens, they were dissolved in acid and analyzed chemically for titanium.

In addition to the magnetic analysis, one end of each specimen was polished, etched, and examined metallographically. The lattice parameter of the polished and etched surface was also obtained, as described below, if the grain size and orientation permitted a rapid determination.

Magnetic Analysis

Curie point measurements were chosen for determining the gamma solvus, in order to minimize the effects of any surface oxidation on the samples during the anneals. Such measurements are nondestructive, are applied to lump samples, and may be used on two-phase or three-phase compositions in which large amounts of the soluble phases are present. In addition, the Curie point is unaffected by grain size, and is practically unaffected by lattice strain (the Curie point of nickel is increased only 2°C under 88,000 psi of pressure (19).)

Marian (20) and Manders (21) have shown that the ferromagnetic and paramagnetic Curie points of nickel solid solutions vary in a linear manner with atomic per cent additions of many elements, and that the change is related to the valence of these elements. To a first approximation,

it appears that the conduction electrons of the solute atoms are contributed to the 3d electron energy band of the nickel, so that when the vacancies in the band are completely filled, the Curie point is lowered to 0° Kelvin. In an alloy, any tendency for the formation of solute-solute bonds, which will remove electrons from association with the nickel lattice, will result in a higher Curie point; thus the Curie point should be a measure of the true solubility of the solute atoms in the solvent lattice.

Measurements were made by recording the pull on a specimen between gradient pole pieces of an electromagnet. Each cylinder, about 1/8 inch by 1/8 inch, was held in a brass cup inside of a thin copper tube, which was noninductively wound with glass insulated constantan wire. Temperatures were measured by copper-constantan thermocouples located at the top, side, and bottom of the specimen. These temperatures were compared with those recorded by a thermocouple located at the center of a hole drilled in a calibration cylinder of pure nickel. The force on the furnace assembly, which contained the sample, was recorded by an analytical balance mounted above the magnet. Horizontal springs, connected to the thermocouple and furnace leads, prevented the assembly from being attracted to either of the poles. The field between the poles was measured with a search coil for different settings of magnet current, and the sample was positioned in the region of maximum field

gradient.

Curves were plotted (against temperature) which were proportional to the magnetic moment per gram, σ :

$$\sigma = \frac{F}{m(dH/dx)} ,$$

where F is the force in grams, m is the mass of nickel present, and dH/dx is the field gradient in oersteds per centimeter. Data were obtained on both heating and cooling at two levels of average field strength, 2100 and 4620 oersteds. Points on these curves were extrapolated against field strength to obtain a curve for zero field, and, according to the method of Weiss and Forrer (22), the square of this curve was extrapolated to zero magnetic moment to give the Curie point.

The uncertainties in temperature measurement, field gradient, and extrapolation resulted in a precision of ± 3°C, which corresponds to ± 0.1 atomic per cent of titanium or carbon in solid solution.

X-Ray Analysis

Most of the lattice parameters were measured using a General Electric XRD-3 high angle spectometer with filtered copper or chromium Kα radiations. Some of the intermetallics were also studied on a Norelco high angle spectrometer with cobalt and iron radiations. The specimens were either crushed to -200 mesh powder and mounted on glass slides, or they were mounted in bakelite, micropolished, and etched to

remove the cold worked layers.

The lattice parameters calculated for the lines of the cubic phases were plotted against $\cos^2 \theta$, and extrapolated to zero ($2\theta = 180^\circ$), in order to minimize eccentricity and absorption errors. When insufficient lines were available to make such an extrapolation, an approximate correction for eccentricity in the specimen holder was made by comparing the 2θ values obtained for a silicon standard in the region under study.

Chemical Analysis

Carbon was analyzed by combustion of chips or powders in a stream of oxygen; the CO_2 obtained was absorbed in ascarite and weighed. Titanium was obtained by dissolving the sample in acid, and forming a precipitate with cupferron. The precipitate was filtered, washed, and ignited, and the TiO_2 obtained was weighed. The result was corrected for nickel or iron carried along in the precipitate by a colorimetric analysis for these elements. The amount of iron present was about 0.05 weight per cent or less. A determination for copper was also made in the samples used for the solvus determination, but the amount present was always 0.01 per cent or less.

Metallography

Polishing was conducted with diamond dust (Diamet Hyprez compound) in kerosene. The back of photographic paper produced less overpolishing and pull-out than any

other lap, although microcloth or miracloth laps were necessary to remove the fine scratches. Rapid wheel speeds and high pressures produced the best results during the preliminary polishing of the harder samples.

Two principal etching reagents were used. A solution of 20 grams of ferric chloride, 8 cc of hydrochloric acid, and 372 cc of ethyl alchol was used for the high nickel compositions. A solution of 25 cc of hydroflouric acid, 25 cc of nitric acid, and 50 cc of glycerine was used to etch titanium and the intermetallics.

Microhardness

The microhardness attachment to a Reichert metallograph was used in identifying phases and in estimating their compositions. Loads between 5 and 80 grams were used, and the diagonal of the square indentation was measured with a calibrated eyepiece attachment. The hardnesses, in kg/mm^2, were plotted against the indentation size on logarithmic coordinate paper, and the resulting straight lines were compared at an indentation diagonal of 10 microns.

DISCUSSION OF RESULTS

Isothermal Section

Figure 2 presents a tentative isothermal section through the ternary at 870°C. The corner positions of the three-phase fields were estimated from the microstructures of the indicated compositions, together with the lattice parameters and microhardnesses of the individual phases. It was found that each of the nickel - titanium binary phases formed two-phase fields with titanium carbide.

Although the equilibrium solubility of nickel in titanium carbide could not be determined with arc cast samples, certain observations indicated that it was very small. The nickel solid solution could be seen in the microstructure of one composition, which contained only 0.80 weight per cent nickel by analysis. Also, the carbide residue obtained by electrolytically leaching a titanium carbide - nickel cermet, which had been sintered four hours at 1350°C (23), contained less than 0.05 weight per cent nickel. The solubility of iron in titanium carbide is also apparently of this order of magnitude, since carbide formed by the menstruum process (24) in a liquid iron solution contains as little as 0.06 weight per cent dissolved iron (25).

The presence of nickel did appear to affect the carbide lattice parameter. The parameter of binary titanium carbide, cast from sponge titanium, varied from 4.30 Angstroms, in the

Figure 2 - Tentative isothermal section at 870°C, showing compositions used for both the isothermal and the solidus measurements near the Ni-Ti binary. Solid circles are compositions made with iodide titanium; open circles are compositions made with sponge titanium.

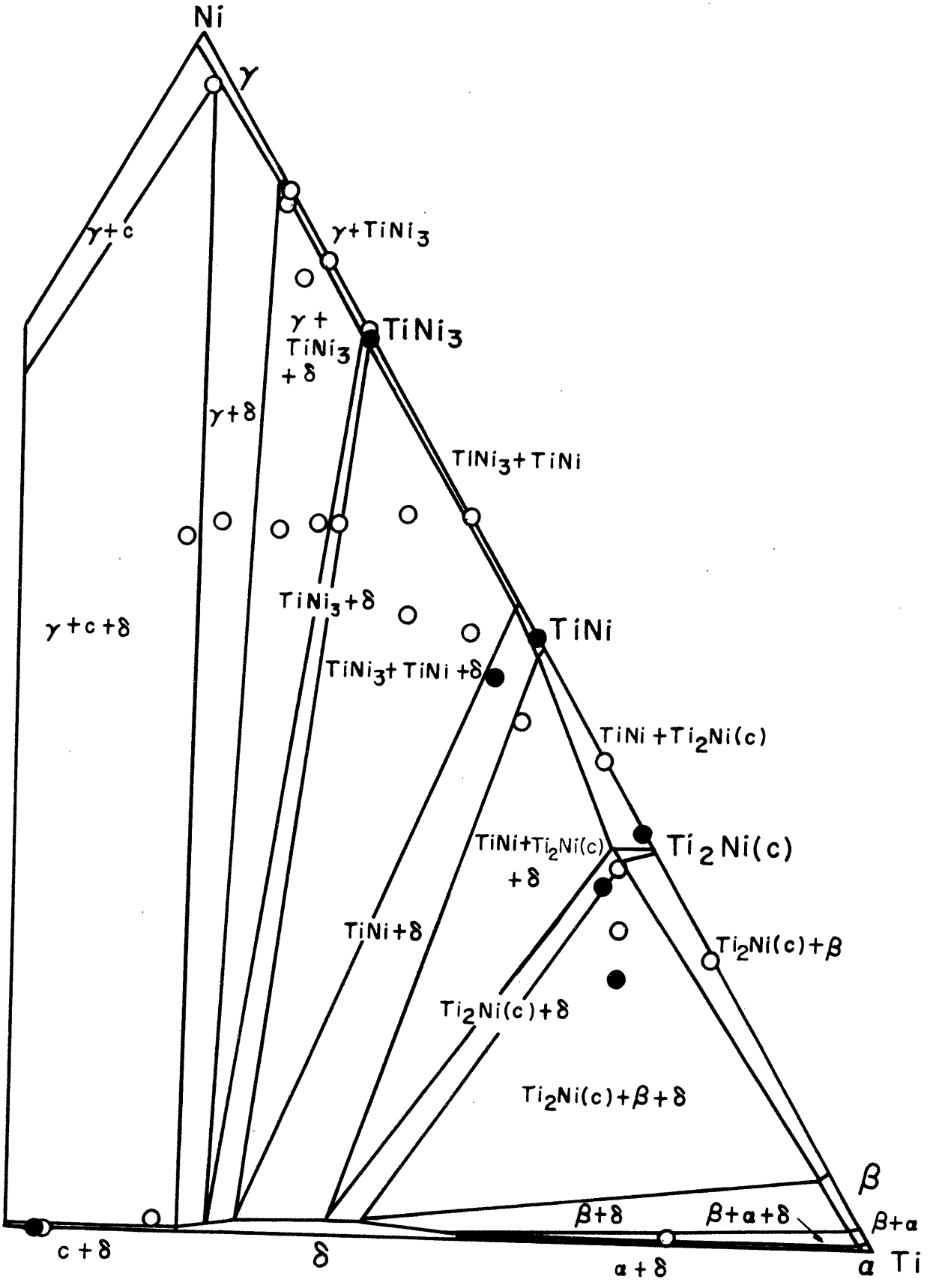
Ni
γ
γ+c
γ+TiNi3
γ + TiNi3 +δ
TiNi3
γ+δ
TiNi3+TiNi
TiNi3+δ
γ+c+δ
TiNi
TiNi3+TiNi+δ
TiNi+Ti2Ni(c)
Ti2Ni(c)
TiNi+Ti2Ni(c) +δ
TiNi+δ
Ti2Ni(c)+β
Ti2Ni(c)+δ
Ti2Ni(c)+β+δ
β
β+δ
β+α+δ
β+α
c+δ
δ
α+δ
α Ti

presence of beta titanium, to 4.3284 ± 0.0005 Angstroms, in the presence of graphite. These results agree well with the variation of parameter with carbon content found by Ragone (26) on sintered carbide prepared from titanium hydride, although the values may be affected by residual oxygen in the sponge. The parameter found on a carbide graphite ingot cast from iodide titanium was 4.3313 ± 0.0003 Angstroms (at 78°F room temperature); Cadoff, Nielsen and Miller (27) reported 4.3316 Angstroms for a stoichiometric carbide similarly prepared.

The ternary samples prepared from sponge in the vicinity of 60 atomic per cent nickel all had about the same parameter, 4.3310 ± 0.0005 Angstroms, even though the microstructures of the analyzed samples indicated that the two-phase boundaries did not extrapolate to the same carbide composition. An ingot cast from nickel shot and TiC powder prepared by Kennametal, Inc. had a parameter of 4.3281 Angstroms, while that of the original powder was 4.3271 Angstroms. The carbides coexisting with TiNi and $Ti_2Ni(C)$ had lower parameters, but the parameters appeared to be higher in the annealed specimens than in the original castings, and there was a tendency for the parameters to increase with increasing annealing temperatures. These results indicate that solution of nickel into titanium carbide produces an increase in lattice parameter.

A similar increase, which was observed when a cermet was annealed for long periods of time, has been explained (28)

TABLE III - CARBIDE HARDNESS AND LATTICE PARAMETER DATA

TITANIUM SOURCE*	OTHER PHASES	ANNEALING TEMPERATURE °C	MICROHARDNESS (± 10 %) kg/mm² 10g load	40g load	10u diagonal	PARAMETER ANGSTROMS
S	α + β	As Cast	1500	1000	1000	4.30 ± .01
I	$Ti_2Ni(C)$+β	As Cast	3800	2500	2000	4.318 ± .001
I	$Ti_2Ni(C)$+β	976	3800	2500	2000	---
S	TiNi+$Ti_2Ni(C)$	870	3400	--	1800	4.32 ± .01
S	TiNi+$Ti_2Ni(C)$	1050	3400	--	1800	4.33 ± .01
I	TiNi	1245	4500	--	2200	4.34 ± .02
S	$TiNi_3$+TiNi	1120	5000	3500	2500	4.3310 ± .0005
S	γ + $TiNi_3$	1285	5000	3500	2500	4.3310 ± .0005
S	C + γ	1260	5000	3500	2500	4.3310 ± .0005
K	γ	As Cast	7000	4000	3000	4.3280 ± .0005
I	C	As Cast	4600	3800	2800	4.3313 ± .0003

* S = Sponge Titanium
I = Iodide Titanium
K = TiC from Kennametal

as the result of "interstitial" solution of nickel in vacant carbon positions of the lattice (NaCl type). Such a mechanism is conceivable, particularly if several carbon vacancies are associated with each nickel atom. Due to the relative metallic radii, a very small amount of nickel dissolved in this way would increase the parameter by the observed amounts.

The microhardness of titanium carbide varied with the composition, and could be determined more easily than the lattice parameter in the low carbide alloys. Table III compares the most significant data. Both the parameters and hardnesses were considered in making the schematic construction in the delta region of Figure 2.

The solution of carbon in $Ti_2Ni(C)$ was estimated from the microstructures of the annealed compositions to be about 3 atomic per cent at 870°C. This is much less than the theoretical composition of 14 atomic per cent, corresponding to Ti_4Ni_2C, and confirms the results of Kuo (29), who could not produce the phase at this composition without the addition of tantalum. In contrast, $Ti_2Ni(O)$ can dissolve up to 10 atomic per cent oxygen at 900°C (12).

The X-ray pattern of $Ti_2Ni(C)$ agreed more closely with the pattern of face centered cubic Ti_2Ni, published by Duwez and Taylor (11), than with the similar structure for Ti_4Fe_2O described by Rostoker (30). The line intensities agreed with those reported by Rautala and Norton (31) and Kiessling (32) for the "theta", or "eta - 2" phase in the

cobalt-tungsten-carbon system.

The lattice was expanded by interstitial additions. The parameter of a ternary composition containing beta and delta, annealed 100 hours at 870°C, was 11.365 ± 0.005 Angstroms. The parameter of binary Ti_2Ni, prepared from iodide titanium, was 11.315 Angstroms, while that prepared from sponge titanium was 11.343 Angstroms. Other values which have been reported for Ti_2Ni are 11.320* (9), 11.333* (11), and 11.29 (30) Angstroms. Values for $Ti_2Ni(O)$ have been reported as 11.30 Angstroms (3) and 11.18 to 11.37 Angstroms (33).

The microhardness of Ti_2Ni, 700 ± 100 kg/mm^2 was increased to 900 kg/mm^2 by the addition of carbon. The structure is extremely brittle, and the ingots containing it split apart spontaneously upon cooling after solidification.

The solubility of carbon in TiNi could not be estimated, since the lattice parameters and microhardnesses were about the same in both binary and ternary alloys at either extreme in composition. As the nickel content increased from stoichiometric TiNi, the parameter decreased from 3.01 ± 0.01 Angstroms to 2.97 ± 0.02 Angstroms at 57 atomic per cent nickel. The microhardness increased, from 300 to 780 kg/mm^2 over the same range.

The solubility of carbon in Ni_3Ti also appeared to be very low. Little difference could be found between the binary and ternary samples prepared from sponge titanium.

---

* Converted from kX units.

However, the sample cast from iodide titanium had slightly lower d values, and it was softer (660 instead of 880 kg/mm^2). Also, the individual plates could be plastically deformed, while the less pure material was brittle.

Solid-Liquid Equilibrium and Solidification

Table IV summarizes the information obtained from the solidus measurements. The data previously obtained for the nickel-titanium binary with (10) and without (9) the possibility of carbon contamination are included for comparison. The exact equilibria temperatures in the region of Ti_2Ni could not be obtained because of oxygen contamination of the liquid during annealing, and because the solidified liquid was sometimes indistinguishable from the solid. However, the peritectic nature of the reaction was established.

The solidus in the nickel corner of the system was studied in detail, since this region is of interest in cermet manufacture. The data obtained on 33 compositions are presented in terms of a 1200°C basal plane projection and three vertical sections (Figures 3, 4, 5A, and 5B). The quasi-binary eutectic between titanium carbide and the nickel solid solution occurs at about 83 atomic per cent nickel (88 weight per cent), and it lies in a plane intersecting the binary at about 9 atomic per cent titanium. The plane between nickel and titanium carbide (Figure 4) contains three-phase fields.

The microstructures encountered during the solidus determination often indicated the changes in the system which

TABLE IV: CONSTANT TEMPERATURE SOLIDUS EQUILIBRIA

BINARY EQUILIBRIUM	TEMPERATURE DEGREES C	TERNARY EQUILIBRIUM	TEMPERATURE DEGREES C
$\frac{L}{\gamma}$	1455 ± 3	$\frac{L}{\gamma + \delta}$	1307 ± 3
$\frac{L}{\gamma + C}$	1325 ± 3	$\frac{L}{\gamma + \delta + C}$	1270 ± 3
$\frac{L}{\gamma + TiNi_3}$	1304 ± 3 (1304)	$\frac{L}{\gamma + \delta + TiNi_3}$	1295 ± 3
$\frac{L}{TiNi_3}$	--- (1380)	$\frac{L + \delta}{TiNi_3}$	1390 ± 15
$\frac{L}{TiNi_3 + TiNi}$	1120 ± 3 (1118)	$\frac{L}{\delta + TiNi_3 + TiNi}$?	1120 ± 3 (1115)
$\frac{L}{TiNi}$	--- (1310)	$\frac{L}{\delta + TiNi}$?	--- (1240)
$\frac{L + TiNi}{Ti_2Ni}$	985 ± 10 (984)	$\frac{L + TiNi + \delta}{Ti_2Ni(C)}$	1050 ± 30 (1015)
$\frac{L}{Ti_2Ni + \beta}$	940 ± 5 (942)	$\frac{L + \delta}{Ti_2Ni(C) + \beta}$	980 ± 10 (955)

Note: Numbers in parentheses in second column are from Reference 9.
Numbers in parentheses in fourth column are from Reference 10.

Figure 3 - 1200°C basal plane projection of the solidus in the nickel corner, showing alloy compositions.

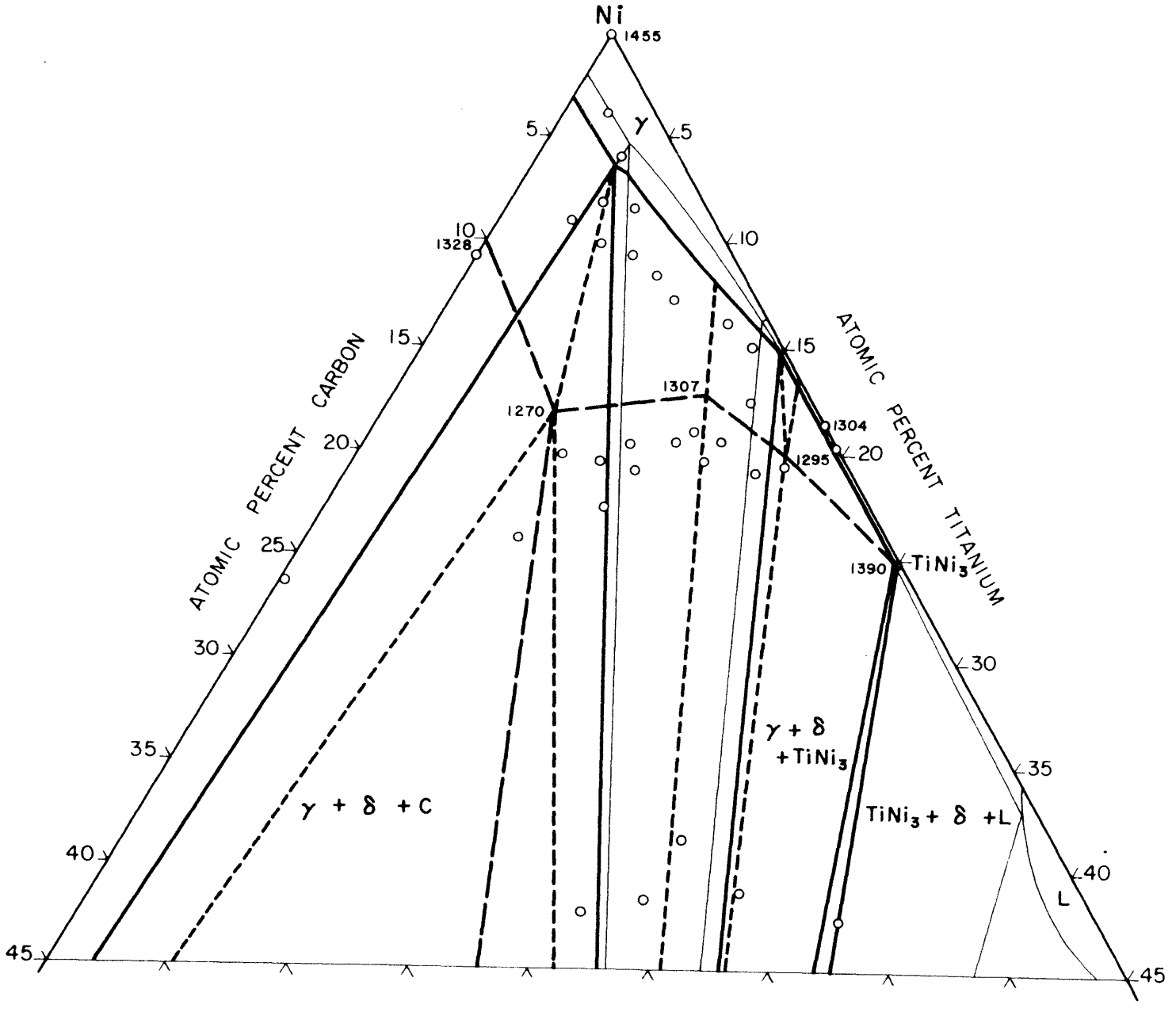
Ni
1455
γ
5
10
1328
15
1307
1270
1304
1295
20
1390
TiNi3
30
35
40
45
L
γ + δ + C
γ + δ + TiNi3
TiNi3 + δ + L
ATOMIC PERCENT CARBON
ATOMIC PERCENT TITANIUM

Figure 4 - Nickel rich portion of the vertical section between nickel and titanium carbide of commercial composition.

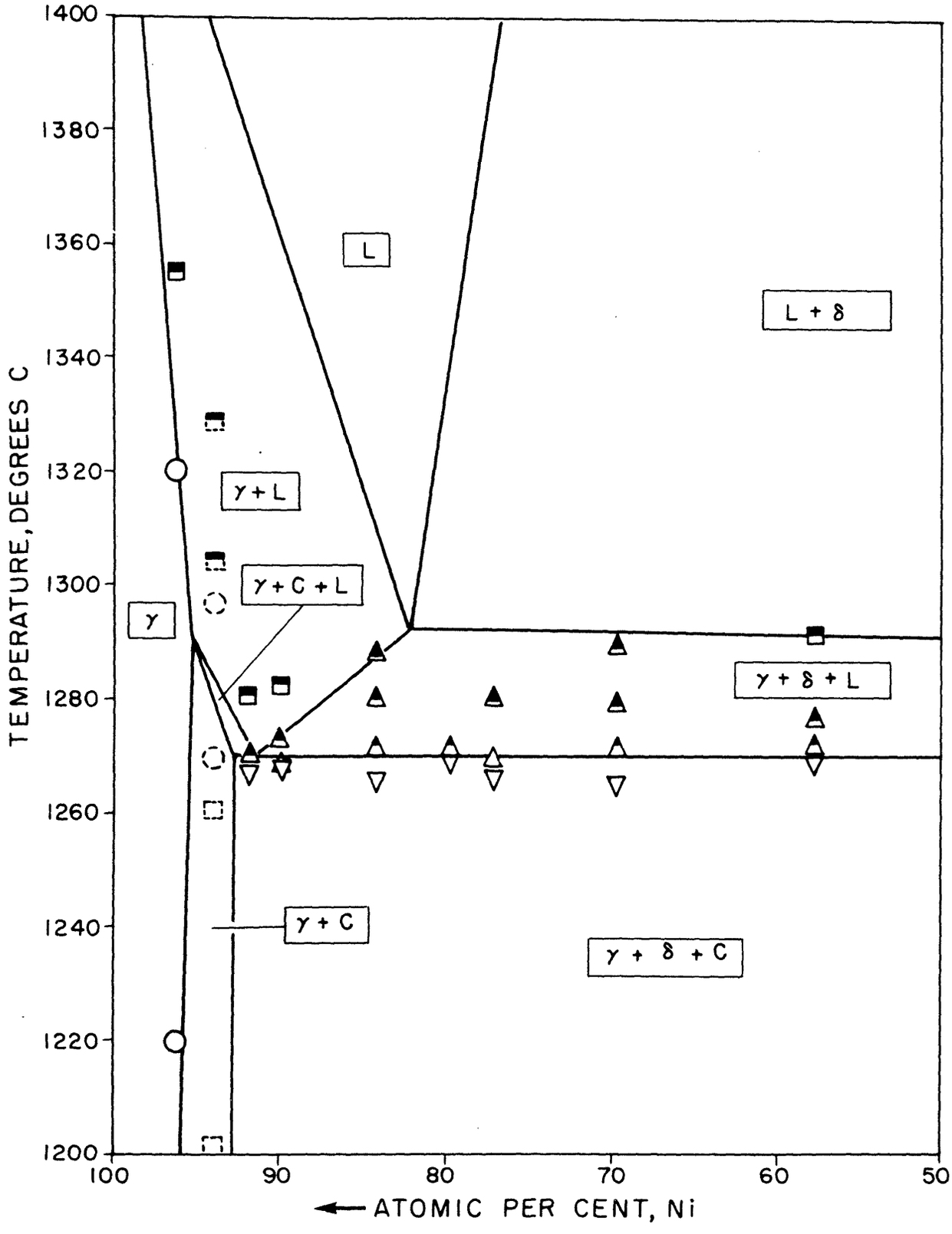
1400
1380
1360
1340
1320
1300
1280
1260
1240
1220
1200
TEMPERATURE, DEGREES C
L
L + δ
γ + L
γ + C + L
γ
γ + δ + L
γ + C
γ + δ + C
100
90
80
70
60
50
← ATOMIC PER CENT, Ni

Figure 5 - Vertical sections intersecting the gamma plus delta field.

A. Section between 7 atomic per cent carbon and 16.4 atomic per cent titanium.

B. Section between 20 atomic per cent carbon and 20 atomic per cent titanium.

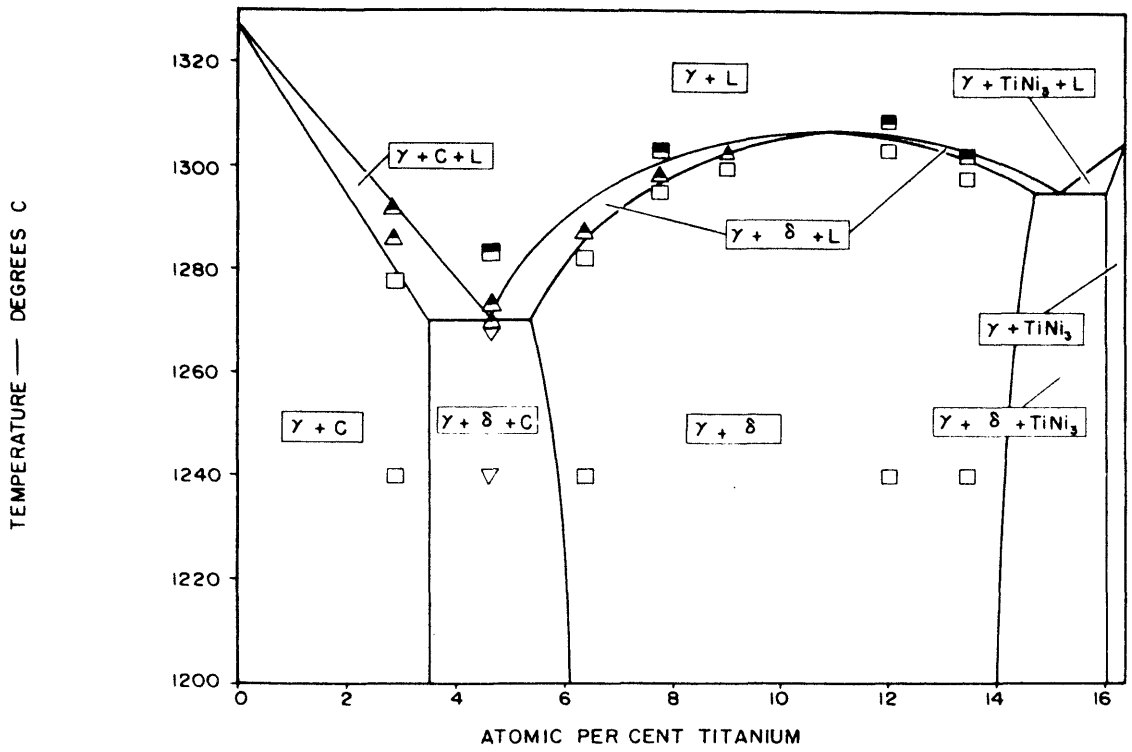
TEMPERATURE — DEGREES C
1320
1300
1280
1260
1240
1220
1200
0
2
4
6
8
10
12
14
16
γ + L
γ + TiNi3 + L
γ + C + L
γ + δ + L
γ + TiNi3
γ + C
γ + δ + C
γ + δ
γ + δ + TiNi3
ATOMIC PER CENT TITANIUM

A

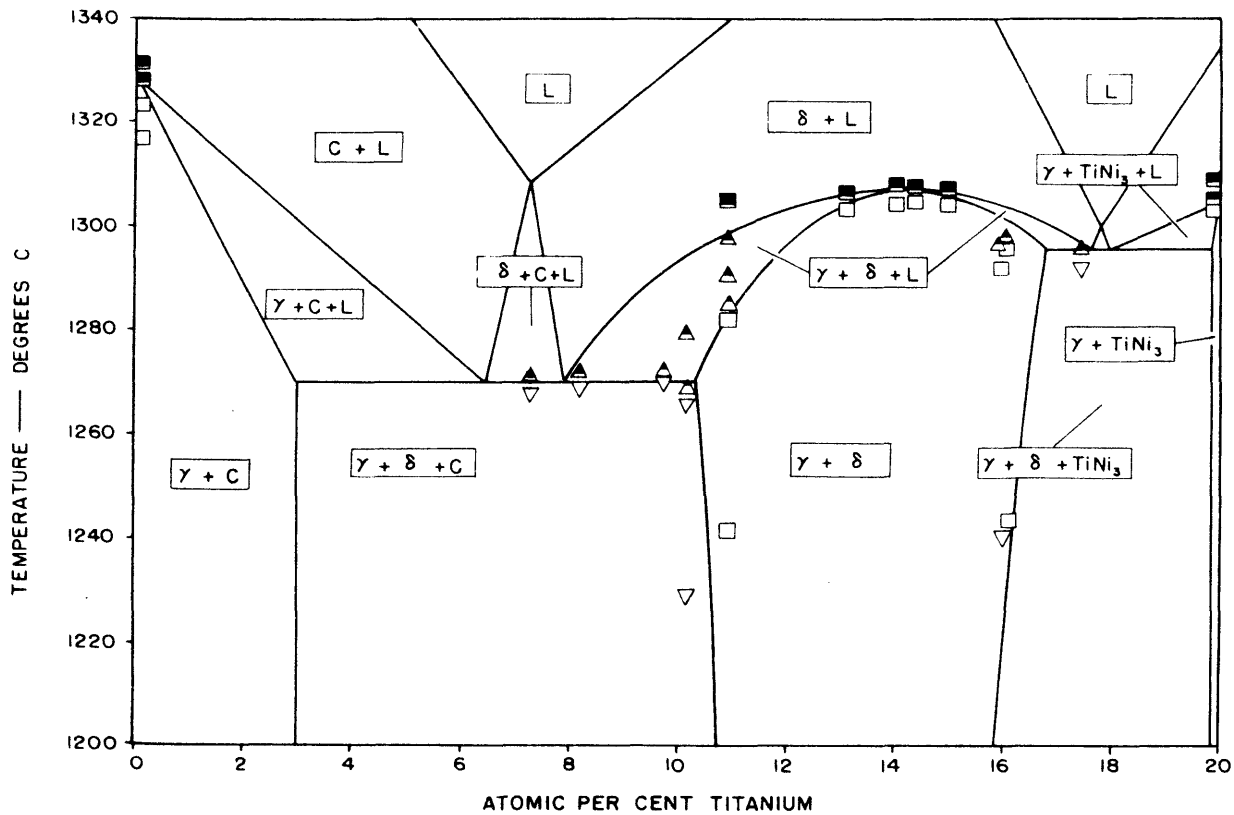
TEMPERATURE — DEGREES C
1340
1320
1300
1280
1260
1240
1220
1200
0
2
4
6
8
10
12
14
16
18
20
L
C + L
δ + L
L
γ + TiNi3 + L
δ + C + L
γ + δ + L
γ + C + L
γ + TiNi3
γ + C
γ + δ + C
γ + δ
γ + δ + TiNi3
ATOMIC PER CENT TITANIUM

B

occur during non-equilibrium solidification. For example, the suppression of the $Ti_2Ni(C)$ peritectic reaction during casting is illustrated in Figure 6. Only a small amount of $Ti_2Ni(C)$ has formed around delta dendrites; the remaining liquid has solidified principally as binary Ti_2Ni, which is etched more rapidly than $Ti_2Ni(C)$, and looks like a separate phase. Figure 7 illustrates the same effect in a similar composition which had been annealed and quenched from just above the solidus; here, the liquid has solidified as both Ti_2Ni and a Ti_2Ni + beta eutectic. The rapidly solidified Ti_2Ni had the same basic X-ray pattern as annealed Ti_2Ni, or $Ti_2Ni(C)$, but there may have been a change of ordering of the atoms within the face centered cubic lattice to produce a different structure.

Other changes due to rapid solidification were observed in the nickel-rich portion of the system. Figures 8 and 9, for example, illustrate a slightly hypereutectic quasi-binary composition after quenching from just below and just above the solidus. The presence of primary nickel dendrites in the quenched liquid structure, together with undissolved carbide, demonstrates that the eutectic composition is shifted to higher carbide contents as the solidification temperature is reduced by rapid cooling.

Figures 10 and 11 illustrate other effects encountered in the gamma + carbon field due to the suppression of graphite nucleation by rapid cooling. The nickel solid solution could be easily supersaturated in carbon, as shown by the micro-

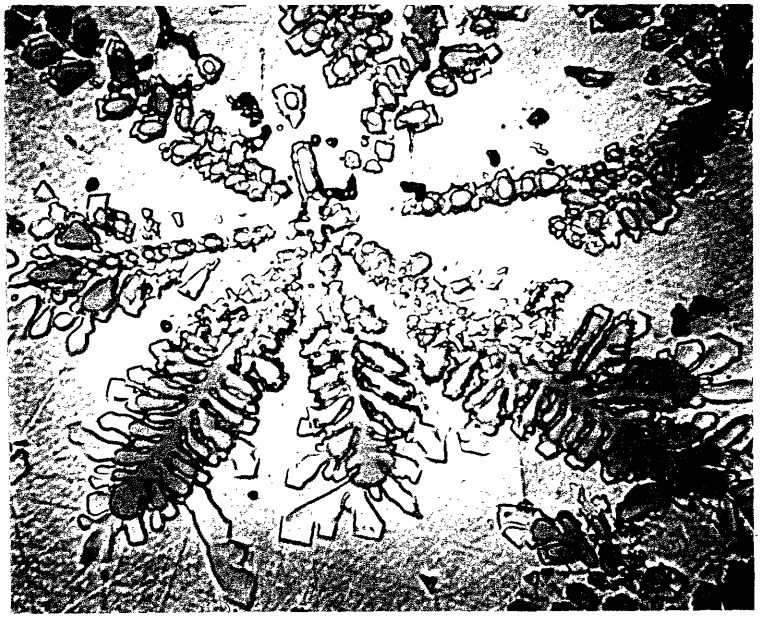

Figure 6 - 66 Ti - 5 C* as cast. Liquid solidified as delta, $Ti_2Ni(C)$, and binary Ti_2Ni. $HF-HNO_3$ etch. 1000 X.

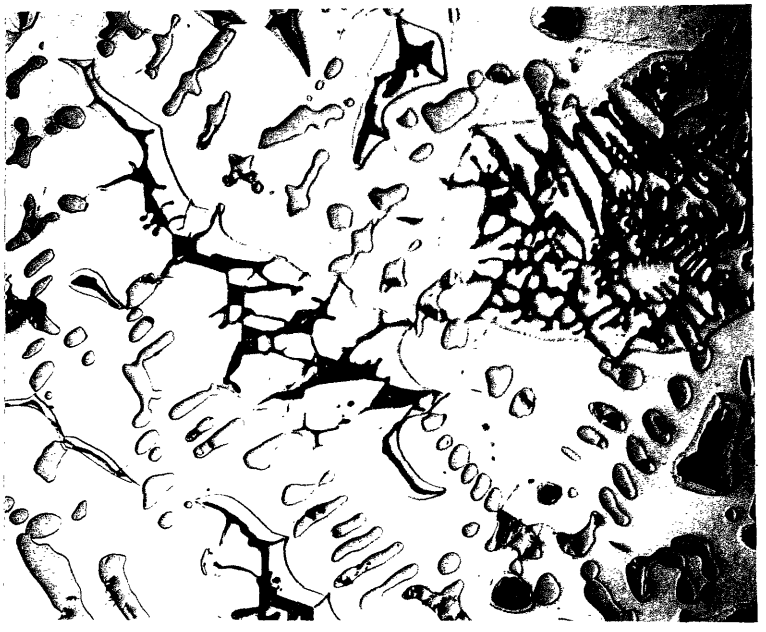

Figure 7 - Nickel rich region of 70 Ti - 8 C* annealed at 1010°C in nickel cup. $Ti_2Ni(C)$ formed by diffusion of nickel into liquid-delta structure. Liquid solidified as Ti_2Ni and Ti_2Ni-beta eutectic. $HF-HNO_3$ etch. 500 X.

*Numbers refer to atomic percentages.

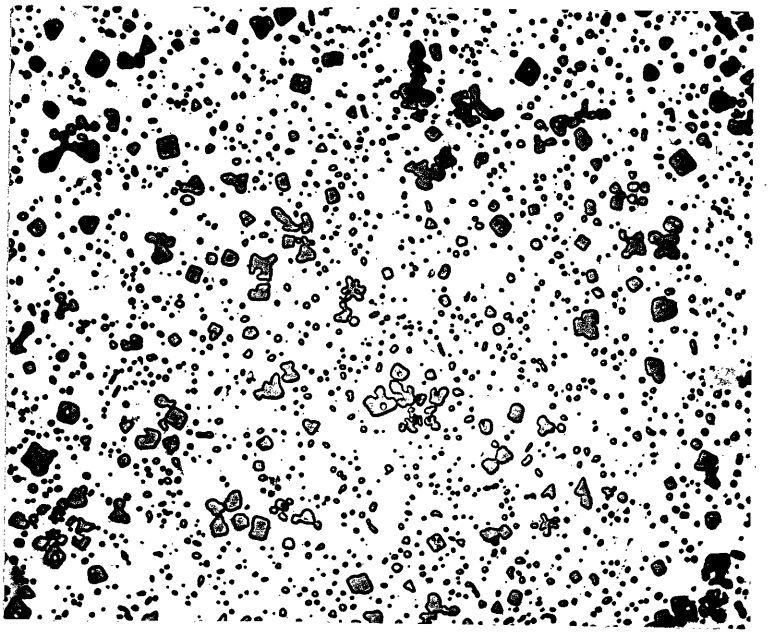

Figure 8 - 13.3 Ti - 5.6 C annealed at 1305°C. Delta plus gamma composition is slightly hypereutectic. $FeCl_3$ etch. 250 X.

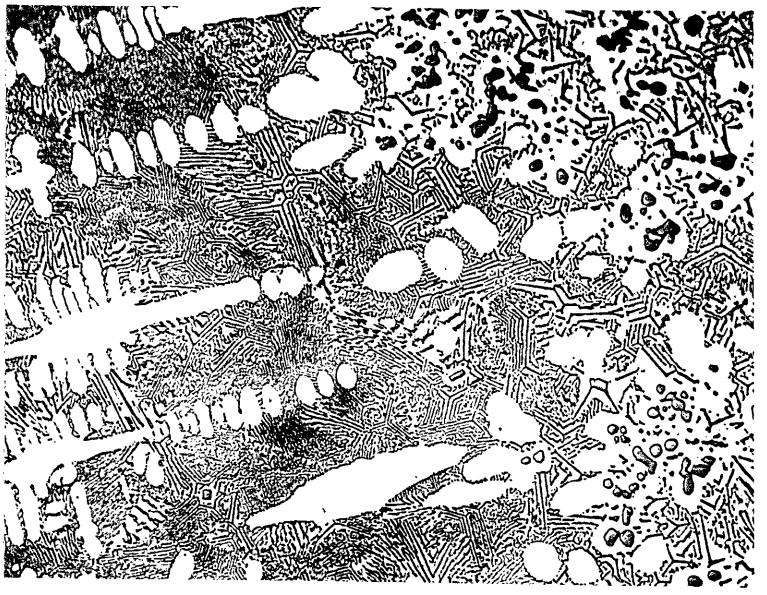

Figure 9 - 13.3 Ti - 5.6 C annealed at 1308°C. Top of sample at right contains undissolved delta. Liquid solidified as primary gamma and gamma-delta eutectic. $FeCl_3$ etch. 250 X.

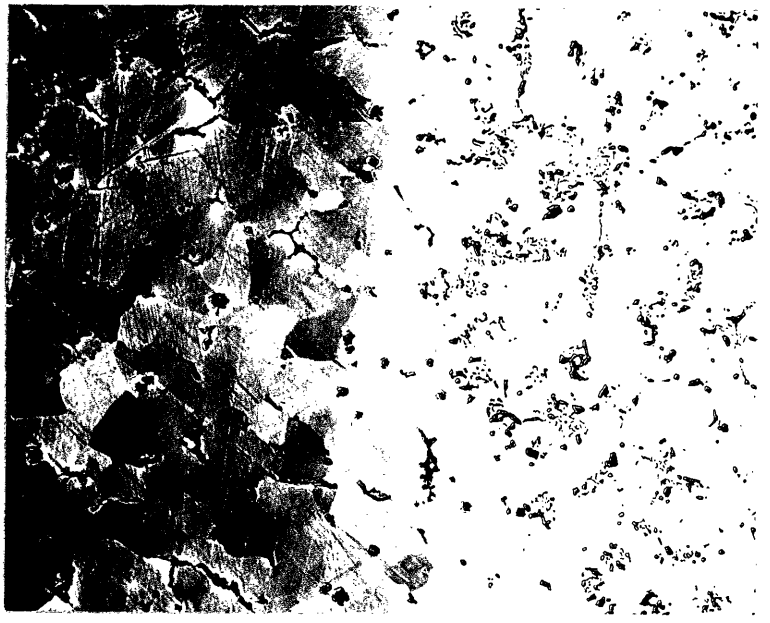

Figure 10 - 10 C - 90 Ni annealed at 1328°C and water quenched. Top of specimen at right was slightly cooler. Bottom of specimen melted. Microhardness of top is 320 kg/mm^2, of bottom, 450 kg/mm^2. $FeCl_3$ etch. 100 X.

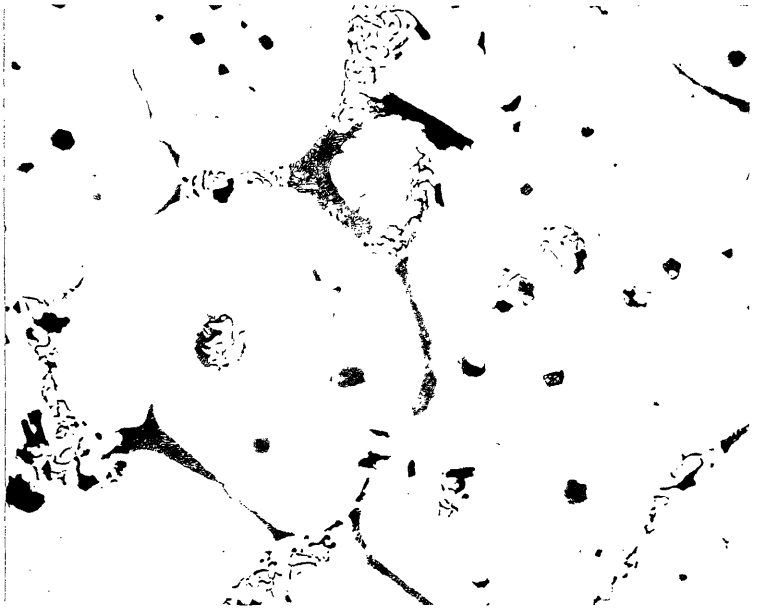

Figure 11 - 2.9 Ti - 6.0 C annealed at 1293°C and water quenched. Liquid in gamma - graphite structure solidified as supercooled graphite eutectic and as an anisotropic carbide eutectic. $FeCl_3$ etch. 300 X.

structure and microhardnesses in a binary sample (Figure 10). When titanium was present, the suppression of graphite formation allowed the precipitation of carbide, even though only graphite was in equilibrium with gamma at the solidus. In the original castings in this region, delta formed on solidification. However, in one sample quenched from just above the solidus (Figure 11), an unidentified carbide phase formed. It is softer than delta and is anisotropic under polarized light.

Precipitation from Nickel Solid Solution

Figure 12 illustrates the results of the magnetic and X-ray measurements in the nickel corner. The sample compositions are indicated by solid circles. An alloy located near the ternary eutectic was also studied. The data points, which are based principally on the Curie points, are shown as open circles. The figure consists of a series of isothermals, between 1260°C and 600°C, and emphasizes the precipitation of graphite from the two-phase field between titanium carbide and the nickel solid solution. Lines of constant Curie point and of constant lattice parameter in the solid solution field are also shown.

The variation of Curie point with composition along the binaries is shown in Figure 13, along with data from the literature for titanium, carbon, and several other quadrivalent elements. The ideal variation for an element contributing four electrons to the 0.61 vacancies in the d

Figure 12 - Data on the precipitation of carbide and graphite from the gamma solid solution. Compositions are indicated by solid circles; data points for the different temperatures are indicated by open circles. Lines of constant Curie point and lines of constant lattice parameter are also indicated.

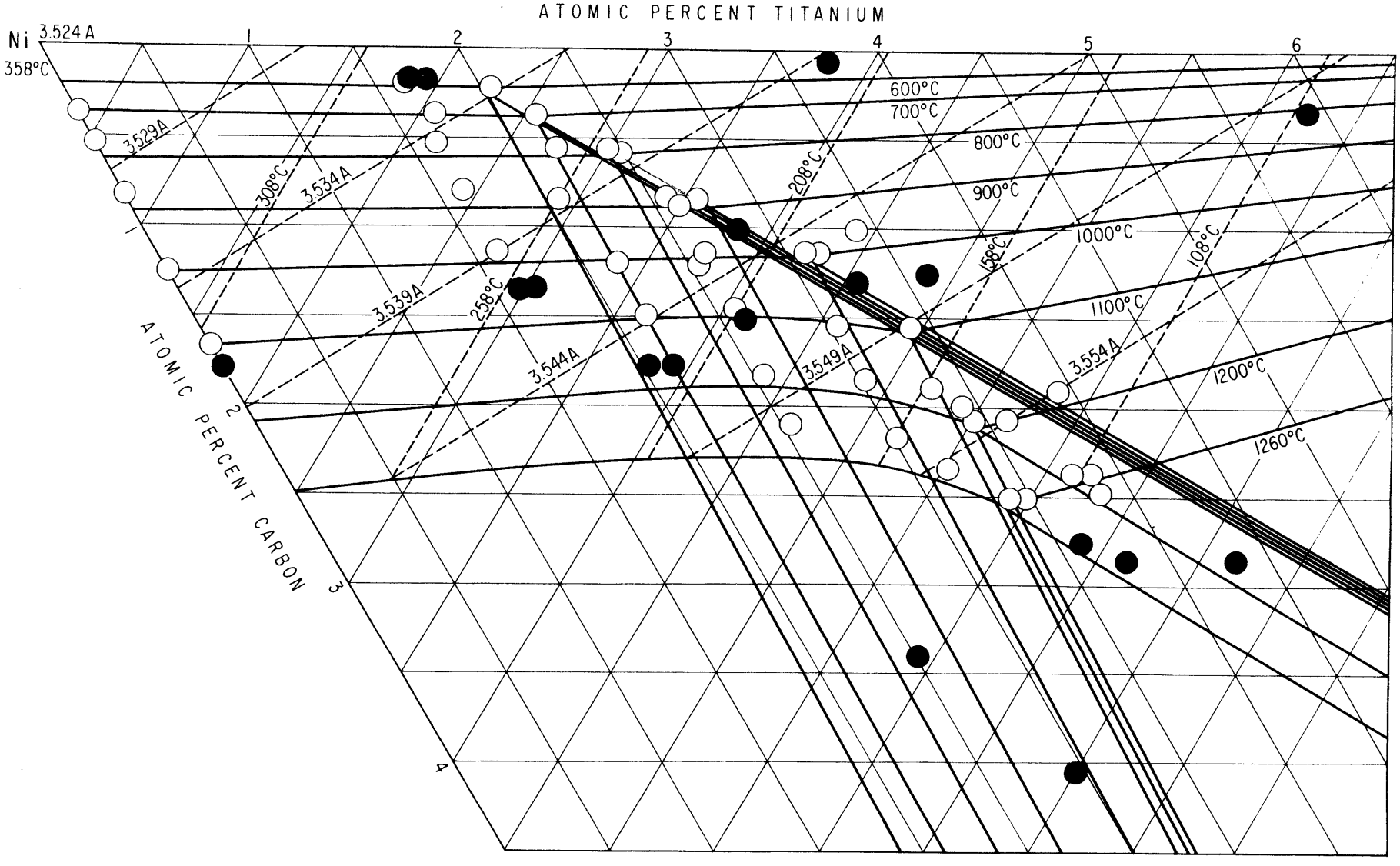
ATOMIC PERCENT TITANIUM
ATOMIC PERCENT CARBON
Ni 3.524 A
358°C
3.529A
308°C
3.534A
258°C
3.539A
3.544A
208°C
3.549A
158°C
108°C
3.554A
600°C
700°C
800°C
900°C
1000°C
1100°C
1200°C
1260°C
1
2
3
4
5
6

Figure 13 - Curie points of quadrivalent binary alloys, compared with the ideal change.

Solid circles - titanium alloys, this investigation.

Open circles labeled C - carbon alloys, this investigation.

K_E - Supersaturated carbon alloys obtained by quenching the liquid. Kase, 1925. (34)

M_E and M_C - Titanium alloys. Marian, 1937. (20)

T - Titanium alloys. Method of obtaining Curie point not stated. Taylor and Floyd, 1952. (35)

$Sn_{E,C}$ - Tin alloys. Marian, 1937. (20)

$Si_{E,C}$ - Silicon alloys. Marian, 1937. (20)

Subscript C refers to the difference between the temperature of the steepest slope on the magnetic moment - temperature curve for the alloy, and that for pure nickel at the same field strength.

Subscript E refers to the difference between the temperature obtained when the slope of the magnetic moment - temperature curve is extrapolated to zero, and the temperature similarly obtained for pure nickel.

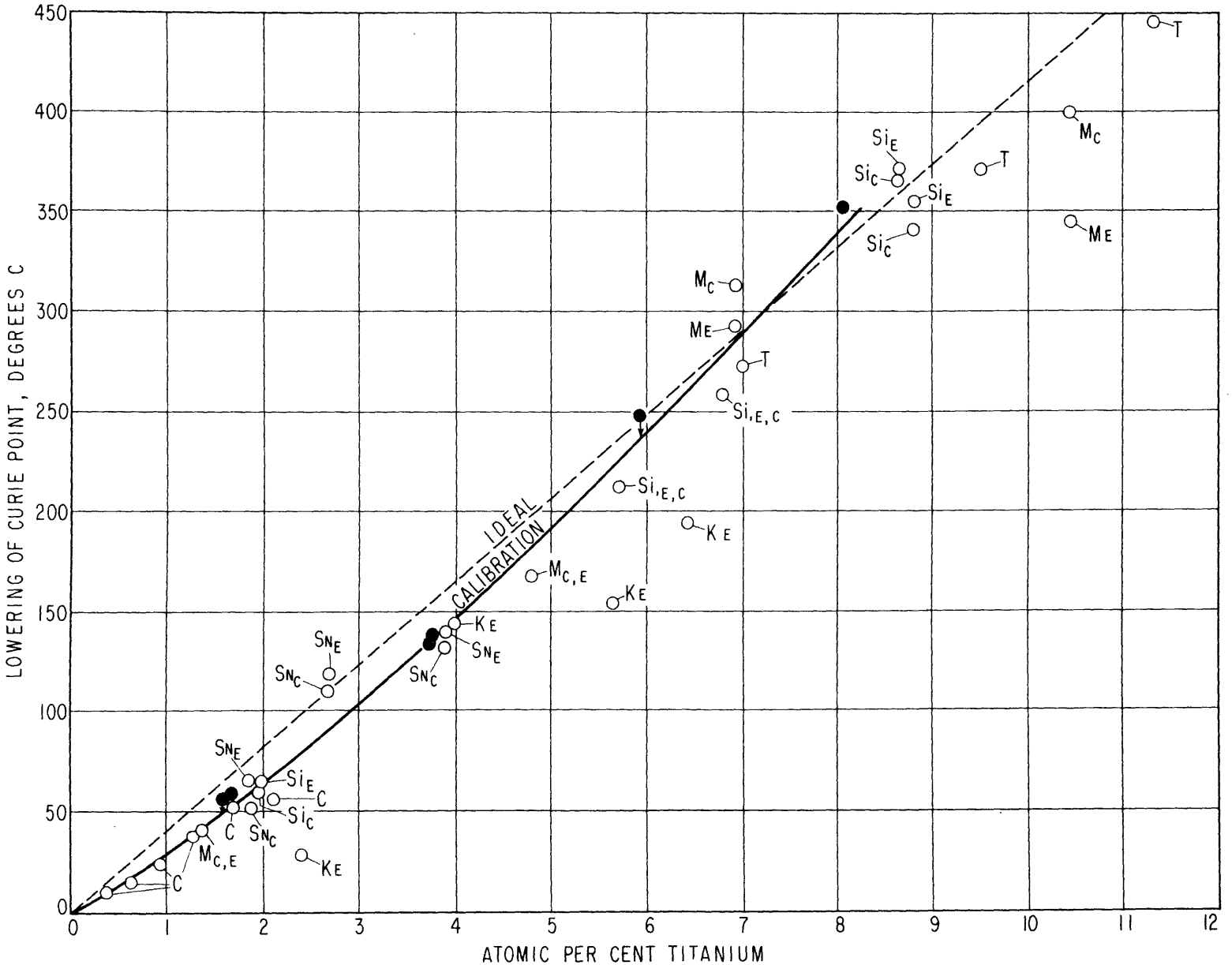
LOWERING OF CURIE POINT, DEGREES C
ATOMIC PER CENT TITANIUM
IDEAL CALIBRATION
0
50
100
150
200
250
300
350
400
450
0
1
2
3
4
5
6
7
8
9
10
11
12
T
MC
SiE
SiC
SiE
T
ME
MC
ME
T
Si,E,C
Si,E,C
KE
MC,E
KE
KE
SNE
SNC
SNE
SNC
SNE
SiE C
SiC
C
SNC
MC,E
KE
C

Figure 14 - Comparison of lattice parameter data obtained on etched surfaces in this investigation with that obtained on powders by Poole and Hume Rothery (9) and Taylor and Floyd (35).

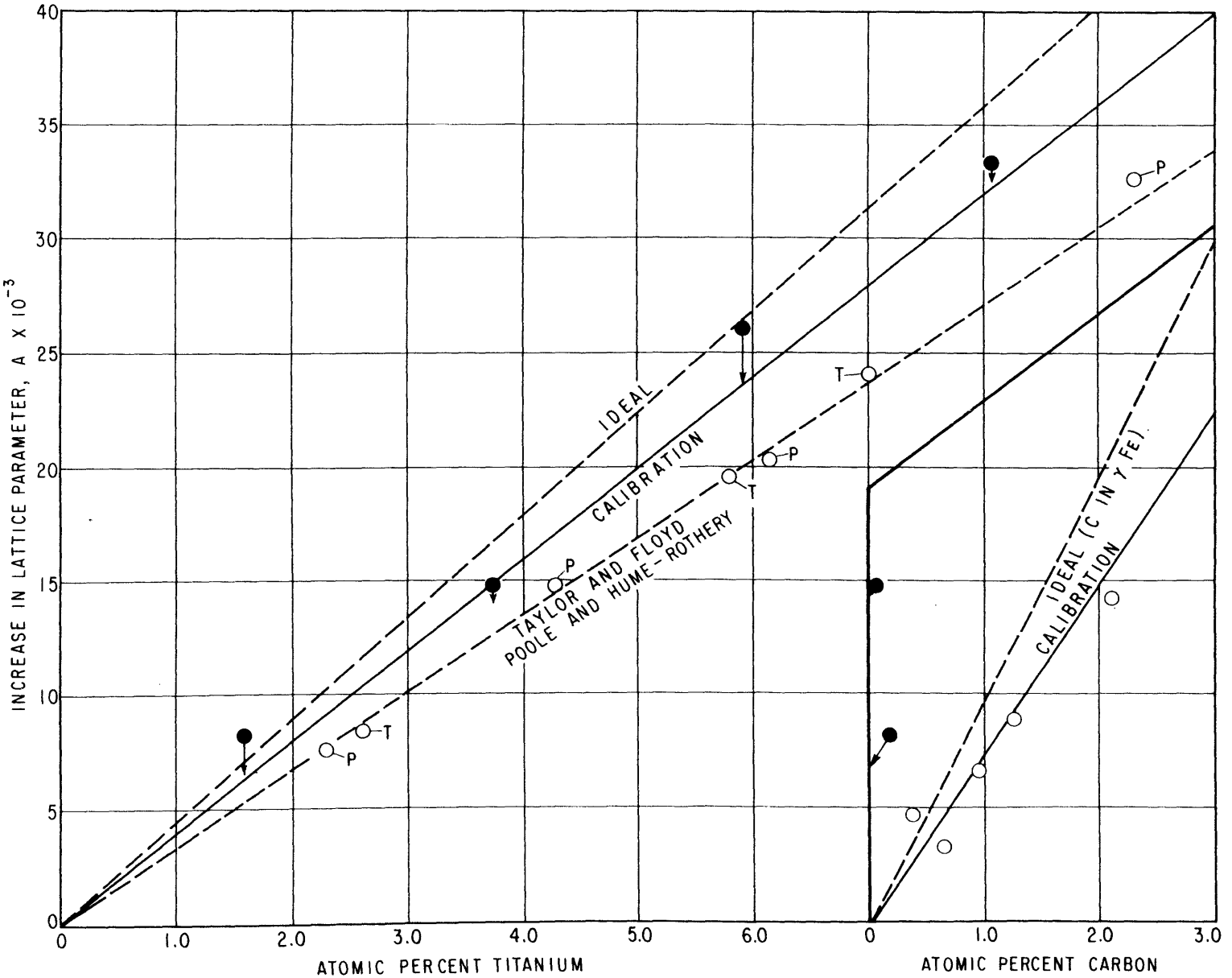
INCREASE IN LATTICE PARAMETER, A X 10^{-3}
ATOMIC PERCENT TITANIUM
ATOMIC PERCENT CARBON
IDEAL
CALIBRATION
TAYLOR AND FLOYD
POOLE AND HUME-ROTHERY
IDEAL (C IN γ Fe)
CALIBRATION
P
T
0
1.0
2.0
3.0
4.0
5.0
6.0
5
10
15
20
25
30
35
40

shell of nickel is also shown. There is a slight negative deviation from the ideal line in the lower composition range, indicating that fewer than four electrons are contributed to the nickel by each solute atom when the amount of solute is small.

The variation of lattice parameter with composition along the binaries is shown in Figure 14. The data were obtained from the polished and etched surfaces of the magnetic samples and are not as precise as previous measurements, (9) and (35), which were made on powders annealed on alundum boats in evacuated capsules. The ideal lines were estimated using Pauling's radii (36) and the lattice parameter variation due to carbon in retained austenite (37) (38).

The accuracy of the isothermals in Figure 12 is limited principally by uncertainties in the analyzed compositions, approximated by the size of the circles, and by any bonding between solute atoms which might have occurred during or after the quench from the annealing temperatures. The more highly alloyed compositions which contained free graphite were observed to age in the vicinity of the Curie point (140 to 200°C) after quenching from 1260°C and 1200°C. When these specimens were kept in liquid nitrogen until the magnetic measurements were made, an incubation time of thirty minutes, or less, was observed before aging began. The aging stopped after several hours, about 0.1 to 0.3

atomic per cent solute having been removed from solution. This aging was not observed in alloys quenched from lower temperatures, and when aging was observed, the Curie point was adjusted by extrapolation on a logarithmic time scale.

The results agree well with the observations of Edwards and Raine (3) that the solubility of titanium carbide in nickel is between 3 and 5 weight per cent at 1250°C. Figure 12 indicates that the true solubility is closer to $2\frac{1}{2}$ weight per cent, and that both graphite and carbide should be present in the structure. However, graphite is not present in their published microstructures, indicating that some carbon may have been lost from the alloys during the vacuum melting of the powder mixtures. If half the carbon were lost from such compositions, an apparent solubility of 5 weight per cent would be expected from Figure 12.

Metallographically it was observed that below 1000°C, the carbide precipitated in a fine dispersion of small particles, while at higher temperatures, only a coarse precipitate developed. Figure 15 illustrates this fine precipitate in the two-phase alloy furthest to the right in Figure 12. Also evident is a differential etching of the solid solution, which may produce the mottled effect often observed in the binder of cermets (39). This etching effect may be related to submicroscopic precipitation or clustering in the solid solution, although no correlation was noticed between this effect and the aging near the Curie point.

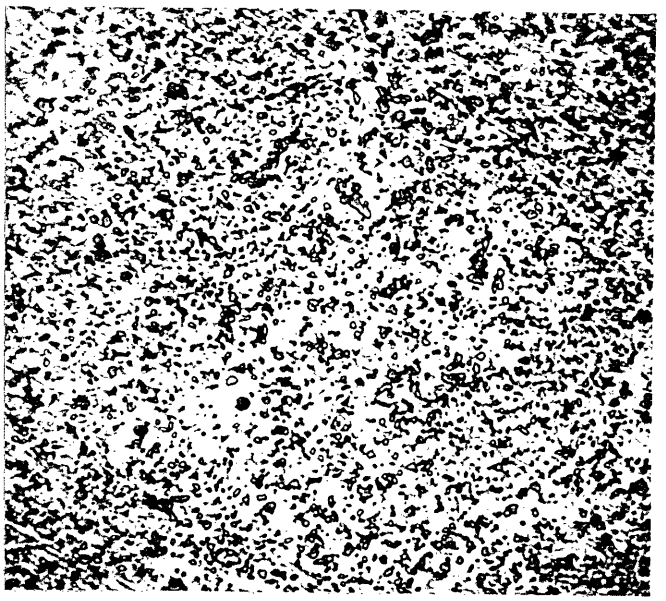

A: Focused on carbide.

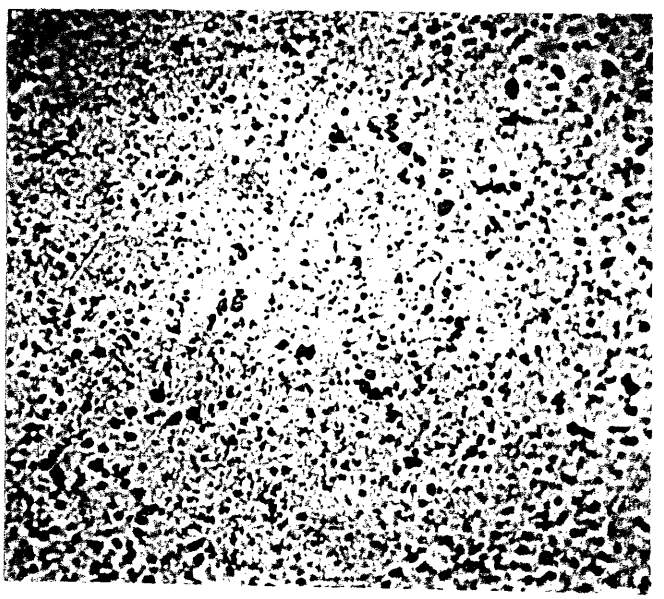

B: Focused on nickel solid solution.

Figure 15 - 4.3 Ti - 2.8 C annealed 1 hour at 1260°C, followed by 400 hours at 700° and 500 hours at 600°C. Fine precipitate observed below 1000°C; also, gamma is attacked to produce a mottled effect. $FeCl_3$ etch. 1500 X.

Arc Cast Grain Structure.

The grain shapes observed in the cast alloys containing nickel solid solution are of some interest, since it has been observed (25) that different grain structures can be obtained in titanium carbide - nickel cermets of similar compositions. Figure 16 illustrates a typical cermet composition arc cast from powders. It may be seen that the irregular carbide dendrites are not completely separated by the nickel, and that the grain size is much larger than is normally desirable. Figure 17 illustrates a more desirable type of structure, which was obtained by carbide segregation in a high nickel ingot.

In the high nickel region, the cast titanium carbide was usually very angular in structure, with highly developed cubic symmetry (Figures 18, 19 and 20). Upon reheating close to the solidus, the corners were rounded, and any eutectic plates were coalesced into spheres (Figure 5). Figure 18 illustrates a eutectic composition slowly cast from a powder mixture in a zirconia crucible. The plates have begun to coalesce due to the slow cooling rate.

Graphite always solidified in the form of plates when oxygen was present, but in the purer arc cast alloys, spheroidal graphite was also observed (Figure 20).

The intermetallic, $TiNi_3$, may be the unidentified third phase observed by Trent and Carter in low carbon cermets (40). It characteristically forms plates in the nickel, either on solidification, or by epitaxial growth

Figure 16 - As cast structure melted from a mixture of powders containing 80 weight per cent TiC and 20 weight per cent Ni. Heavily etched with $FeCl_3$ reagent. 100 X.

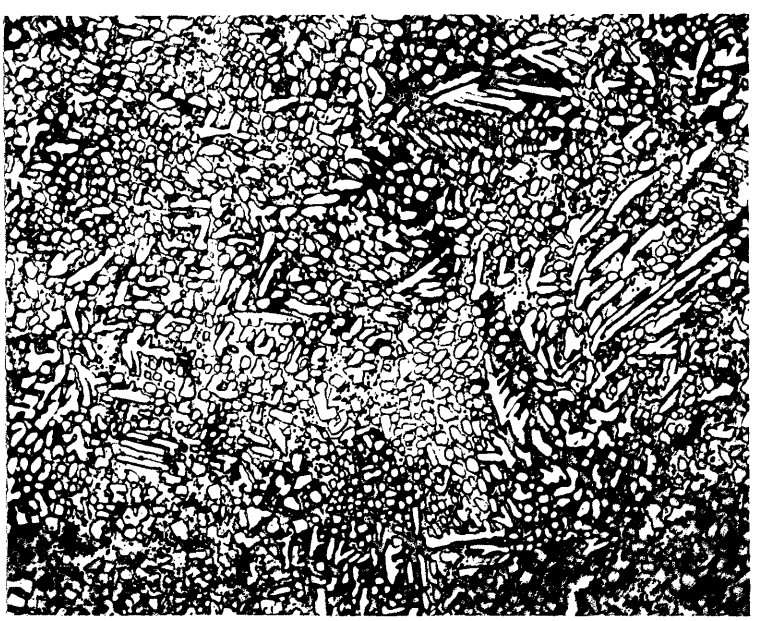

Figure 17 - Carbide rich region in segregated alloy containing 18.5 atomic per cent C and 22.9 atomic per cent Ti, annealed at 1305°C and quenched. Heavily etched with $FeCl_3$ reagent. 100 X.

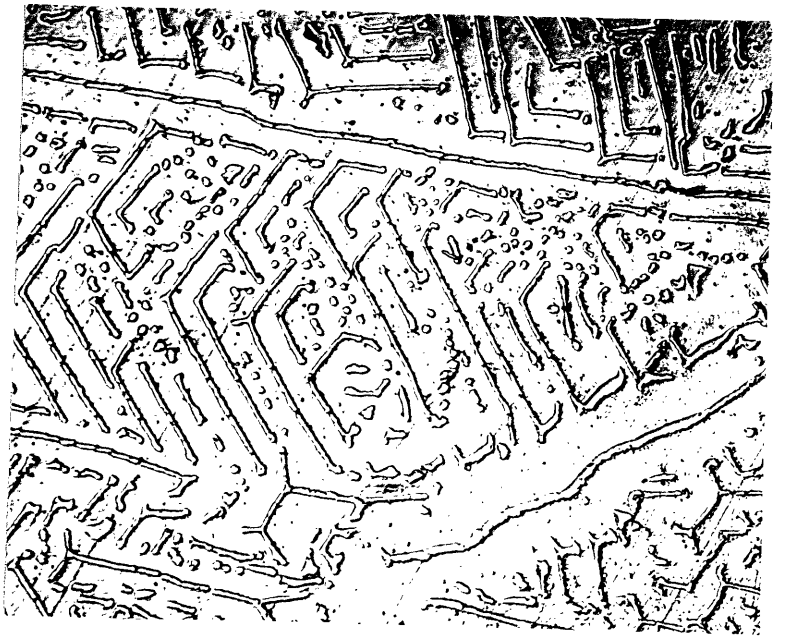

Figure 18 - Eutectic structure in lower half of a slowly cooled casting made by melting a powder mixture containing 14.3 weight per cent titanium carbide in a zirconia crucible. $FeCl_3$ etch. 500 X.

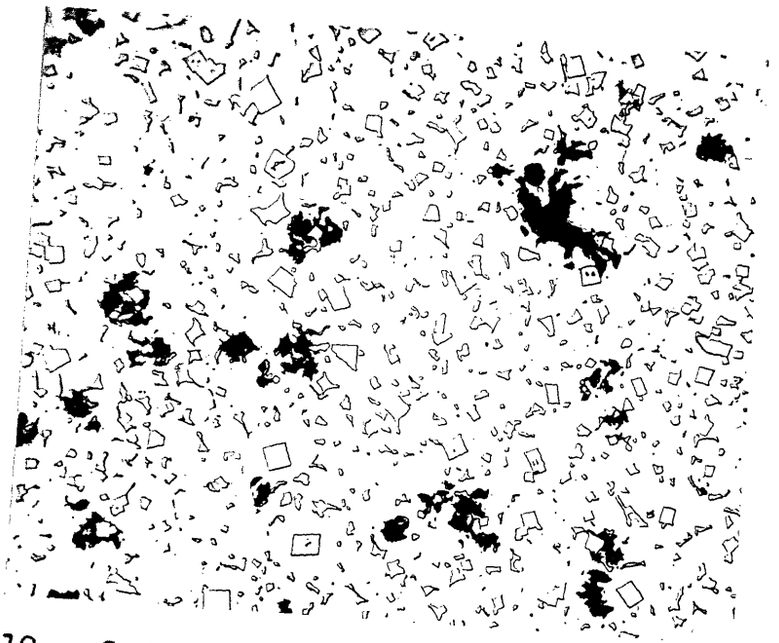

Figure 19 - 8.4 Ti - 11.8 C as cast. Composition is close to ternary eutectic, gamma - delta - graphite. $FeCl_3$ etch. 350 X.

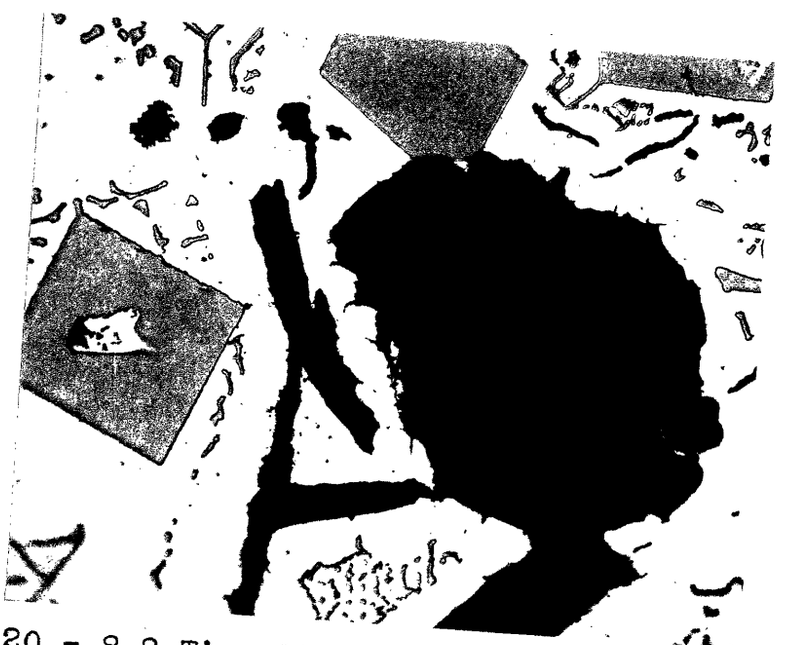

Figure 20 - 8.8 Ti - 15.3 C as cast. Liquid solidified as a graphite spherulite, graphite plates, primary delta, and eutectic structures. $FeCl_3$ etch. 1000 X.

Figure 21 - 17.8 Ti - 2.8 C annealed at 1284°C. Carbide eutectic structure has coalesced, but $TiNi_3$ plates have not. $FeCl_3$ etch. 300 X.

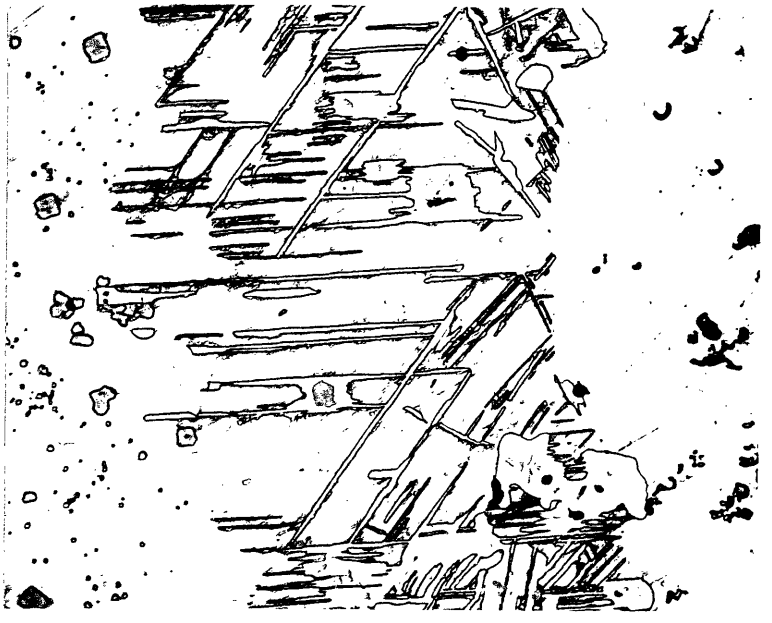

Figure 22 - 16.6 Ti - 4.0 C annealed at 1280°C in an unusually impure atmosphere. Carbon has diffused out of the equilibrium gamma - delta structure to produce a region of gamma - delta - $TiNi_3$ and a region of gamma - oxide. $FeCl_3$ etch. 300 X.

from the nickel solid solution, and, as Figure 21 illustrates, it is not readily coalesced by annealing. It can also be formed by decarburizing the nickel solid solution under certain circumstances, as indicated in Figure 22.

Effects of Oxygen.

Some of the effects of oxygen on the microstructure in the gamma region were examined on preliminary samples, which had been prepared by melting powder mixtures in zirconia crucibles. Several ingots, which were arc cast from powder mixtures containing increasing amounts of NiO, were also studied.

It was found that at high temperatures in the liquid, oxygen in solution reacted with the carbon to form a gas, resulting in considerable porosity, and a progressive decarburization of the liquid until only oxide phases existed with the nickel solid solution after cooling. At lower temperatures, during slow cooling in oxide crucibles, oxygen partially replaced carbon in the carbide lattice, producing graphite on solidification and decreasing the solubility of the carbide in the liquid. The latter effects are illustrated in Figures 23 and 24. The presence of oxygen in the carbide was often associated with dark grey regions, resembling stains, on the carbide surfaces in the microstructure; a pink tint to the grains was associated with nitrogen contamination.

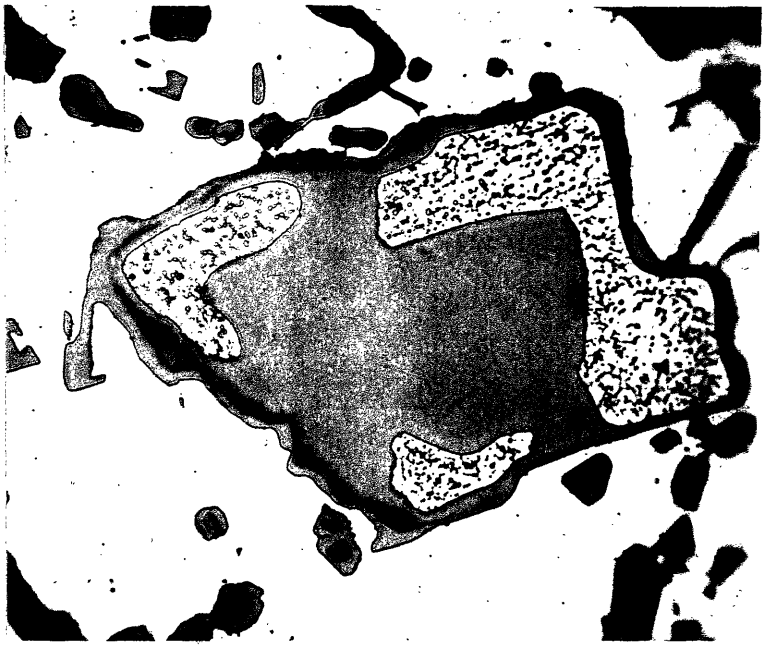

Figure 23 - Partially dissolved carbide grain in an ingot prepared by melting a powder mixture, containing 13.7 weight per cent TiC, in a zirconia crucible under tank argon. Discoloration in undissolved shell was associated with oxygen. $FeCl_3$ etch. 1000 X.

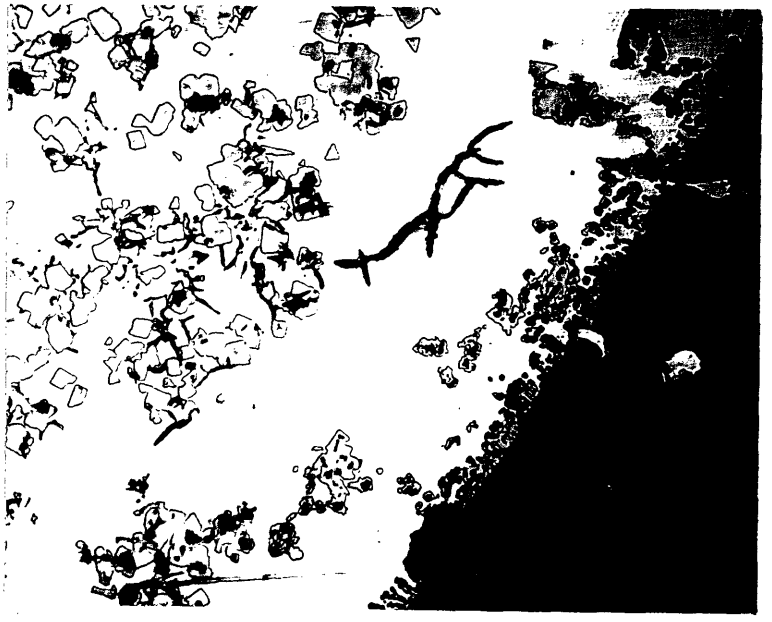

Figure 24 - Structure near crucible wall in ingot made by melting a 10 weight per cent TiC, 90 per cent Ni powder mixture, and slowly cooling. Oxygen has dissolved in the TiC and produced graphite flakes on solidification. (Center of ingot contained a coarse eutectic, not evident here.) $FeCl_3$ etch. 350 X.

CONCLUSIONS

The ternary phase relations determined here reveal several facts about pure titanium carbide - nickel cermets. The binder phase in such alloys, unlike that in tungsten carbide - cobalt compositions (31) can dissolve the carbide forming element almost to the limit of binary solubility; thus binders of different mechanical properties may be used. Graphite can form unless the binder contains 2 atomic per cent more titanium than carbon in solid solution. Plates of Ni_3Ti may occur if the carbide phase contains much less than the stoichiometric amount of carbon; however, the more brittle eta-type structure, which is easily obtained in tungsten carbide - cobalt alloys, cannot coexist with the nickel solid solution.

During sintering or infiltration, a low-titanium nickel binder will dissolve at least 17 atomic per cent titanium plus carbon when liquid, and it will melt or solidify over some range of temperatures between 1270°C and 1307°C. It is possible to sinter most high-binder compositions in the presence of both solid and liquid binder. Oxygen contamination is deleterious during sintering, not only because of gas formation at the higher temperatures, but because it reduces the solubility of titanium carbide in the liquid and promotes the precipitation of graphite plates.

Heat treatment below the solidus may be used to spheroidize angular carbide particles and to control the

precipitation of carbide and graphite from the solid solution. Graphite can start to precipitate on cooling certain gamma - carbide compositions between 1270°C and 1000°C, as shown in Figure 12. Precipitation of both carbide and graphite can occur in a finely divided form below 1000°C. The solubility of carbon in the binder is similar to the solubility in pure nickel, and most of the carbon may be removed from solution by heating at low temperatures.

In future studies of the changes taking place during heating below the solidus, it may be useful to compare the changes in Curie point with the simultaneous changes in lattice parameter. Since the two properties vary differently within the solid solution, the binder composition changes in the ternary solid solution may be followed.

Microstructures similar to those observed in cermets may be obtained by arc casting; however, the large grain size and segregation encountered would result in inferior properties. Except at a composition of about 10 weight per cent carbide, cermet casting is probably not practical.

SUMMARY

The system nickel-titanium-carbon has been studied on samples arc cast in helium, using metallographic, magnetic, X-ray and microhardness measurements. It was found that titanium carbide forms two-phase fields with each of the nickel-titanium binary phases. The eta-2 structure, Ti_2Ni, dissolves at 870°C about 3 atomic per cent carbon, which increases the lattice parameter and microhardness. TiNi and $TiNi_3$ dissolve very little carbon. Nickel dissolves into titanium carbide to a very limited extent, but it causes a measurable lattice expansion.

Solidus temperatures in the vicinity of Ti_2Ni are increased by additions of carbon, and $Ti_2Ni(C)$ forms by a peritectic reaction between liquid and titanium carbide. The solidus in the vicinity of nickel, however, is lowered; a quasi-binary eutectic occurs at about 13 atomic per cent titanium and 4 atomic per cent carbon (at 1307°C). Two ternary eutectics, which produce a nickel solid solution, titanium carbide, and either graphite (at 1270°C), or $TiNi_3$ (at 1295°C) also occur. The plane between nickel and titanium carbide cuts through three-phase fields containing liquid or graphite.

The atomic per cent solubility in nickel of titanium carbide, together with graphite, was determined from the Curie points in the nickel solid solution as follows: 3.4 titanium plus 2.6 carbon at 1260°C, 3.1 titanium plus 1.2

carbon at 1000°C, and less than 2.0 titanium plus 0.2 carbon at 600°C. Graphite will precipitate from the binder of a pure ternary cermet at 1000°C or below, unless the binder contains 2 atomic per cent more titanium than carbon in solution.

In the microstructure, angular titanium carbide particles may be formed by rapid solidification of high purity alloys, but these particles will tend to spheroidize upon annealing close to the solidus. Although $TiNi_3$ always appears in the form of plates, graphite will form as spheroidal particles instead of plates, if the oxygen content of the liquid is low. Cermet-like microstructures may be obtained by arc casting titanium carbide - nickel compositions, but the particle size is large, and carbide segregation is difficult to avoid.

Oxygen dissolved in titanium carbide decreases the solubility of the carbide in liquid nickel. It also causes graphite precipitation near the solidus and can result in alloy decarburization, through gas formation, at higher temperatures.

ACKNOWLEDGEMENTS

The author wishes to express his sincere appreciation to Professor John Wulff for his continued support, and very helpful advice and criticism, in patiently guiding this research.

Among the many other persons who have contributed to the success of this work, the author is particularly indebted to Mr. Donald Guernsey, who supervised the chemical analyses, and to Mr. Su T. Lin, who made possible the magnetic field calibration.

The author also wishes to express his appreciation to the General Electric Company for the fellowship under which a major portion of this work was done. Support was also obtained from Air Force contract No. AF 33(616)-61, and the Massachusetts Institute of Technology.

REFERENCES

1. For example, see: G. M. Ault and G. C. Deutsch: Applicability of Powder Metallurgy to Problems of High Temperature Materials. Also, discussion. Trans AIME (1954) 200, pp 1214-1230.

2. N. M. Zarubin and L. P. Molkov: Investigations of Alloys Produced According to Ceramic Methods. Vestnik Metalloprov (1935) 15, pp 93-98; Chemical Abstracts 31, 6170

3. R. Edwards and T. Raine: The Solid Solubilities of Some Stable Carbides in Cobalt, Nickel, and Iron at 1250°C. Plansee Proceedings "De Re Metallica," 1952. Metallwerk Plansee Ges. M.B.H. Reute, Tyrol. 1953. p 232.

4. E. R. Stover and J. Wulff: Studies in the System Nickel-Titanium-Carbon. WADC Technical Report 54-212. M.I.T. January 1954; also, E. R. Stover: The Binder Phase in Titanium Carbide - Nickel Cermets. S. M. Thesis, M.I.T. Department of Metallurgy, 1952.

5. M. Hansen: Der Aufbau der Zweistofflegierungen. Julius Springer, Berlin, 1936. pp 380-381.

6. H. Morrogh and W. J. Williams: Graphite Formation in Cast Irons and in Nickel-Carbon and Cobalt-Carbon Alloys. Jnl Iron and Steel Inst (1947) 155, pp 322-369.

7. J. J. Lander, H. E. Kern, and A. L. Beach: Solubility and Diffusion Coefficients of Carbon in Nickel; Reaction Rates of Nickel-Carbon Alloys with Barium Oxide. Jnl Appl Phys (1952) 23, p 1305.

8. T. E. Kihlgren and J. T. Eash: Carbon Nickel System. Metals Handbook, 1948 Edition, American Society for Metals, p 1183.

9. D. M. Poole and W. Hume-Rothery: The Equilibrium Diagram of the System Nickel-Titanium. Jnl Inst Metals (1955) 83, pp 473-480.

10. H. Margolin, E. Ence, and J. P. Nielsen: Titanium-Nickel Phase Diagram. Trans AIME (1953) 197, pp 243-247.

11. P. Duwez and J. L. Taylor: The Structure of Intermediate Phases in Alloys of Titanium with Iron, Cobalt, and Nickel. Trans AIME (1950) 188, p 1173.

12. W. Rostoker: Selected Isothermal Sections in the Titanium-Rich Corners of the Systems Ti-Fe-O, Ti-Cr-O, and Ti-Ni-O. Trans AIME (1955) 203, pp 113-116.

13. J. G. McMullin and J. T. Norton: The Ternary System Ti-Ta-C. Trans AIME (1953) 197, pp 1205-1208.

14. I. Cadoff and J. P. Nielsen: Titanium-Carbon Phase Diagram. Trans AIME (1953) 197, pp 248-252.

15. G. A. Meerson and O. E. Krein: Investigation of the Mechanism of the Formation of Titanium Carbide in Vacuo. Zhurnal Prikladnoi Khimii (1952) 25, pp 134-147; Henry Brutcher Translation No. 3121.

16. K. Becker: The Physical Characteristics of High-Melting Compounds. Physikalische Zeitschrift (1933) 34, pp 185-198.

17. P. Schwartzkopf and R. Kieffer: Refractory Hard Metals, MacMillan, New York, 1953, p 87.

18. F. W. Glaser and W. Ivanick: Sintered Titanium Carbide. Trans AIME (1952) 194, pp 387-390.

19. L. Patrick: The Change of Ferromagnetic Curie Points with Hydrostatic Pressure. Physical Review (1954) 93, pp 384-391.

20. V. Marian: Ferromagnetic Curie Points and the Absolute Saturation of Some Nickel Alloys. Annales de Physique (1937) 7, pp 459-527.

21. C. Manders: Paramagnetic Study of Several Alloys of Nickel. Annales de Physique (1936) 5, pp 167-231.

22. P. Weiss and R. Forrer: Spontaneous Magnetization of Nickel. Comptes Rendus (1924) 178, pp 1670-1673.

23. R. G. Bourdeau, personal communication, M.I.T. 1952.

24. P. M. McKenna: Process for Making Titanium Carbide. U.S. Patent 2,515,463, July 18, 1950.

25. H. Blumenthal and R. Silverman: A Study of the Microstructure of Titanium Carbide. Trans AIME (1955) 203, pp 317-322.

26. D. V. Ragone: S.B. Thesis, M.I.T. Department of Metallurgy, 1951.

27. I. Cadoff, J. P. Nielsen, and E. Miller: Properties of Arc Melted Versus Powder Metallurgy Titanium Carbide. Seminar on "High-Temperature and Corrosion Resistant Materials by Powder Metallurgy," held in Reutte/Tyrol, Austria - June 19-23, 1955; Abstracts of Papers circulated by W. B. Crandall, Alfred University, Alfred, N.Y.

28. A. D. Joseph, R. P. Rieget, V. D. Scheffer, and J. R. Tinklepaugh: The Heat Treatment, Reinforcement, and Cladding of Titanium Carbide Cermets. WADC Technical Report 55-82, December 1954, New York State College of Ceramics, Alfred University.

29. K. Kuo: Triple Eta$_2$ Carbides and the Atomic Size Factor. Acta Metallurgica (1953) 1, pp 611-613.

30. W. Rostoker: Observations on the Occurrence of Ti_2X Phases. Trans AIME (1952) 194, pp 209-210.

31. P. Rautala and J. T. Norton: Tungsten-Cobalt-Carbon System. Trans AIME (1952) 194, p 1045.

32. R. Kiessling: discussion to P. Rautala and J. T. Norton, above, Trans AIME (1953) 197; Jnl of Metals, May 1953, p 745.

33. N. Karlsson: Metallic Oxides with the Structure of High-Speed Steel Carbide. Nature (1951) 168, p 558.

34. T. Kase: On the Equilibrium Diagram of the Iron-Carbon-Nickel System. Science Reports of the Tohoku Imperial University, Japan, Series I, (1925) 14, pp 174-219.

35. A. Taylor and R. W. Floyd: The Constitution of Nickel-Rich Alloys of the Nickel-Chromium-Titanium System. Jnl Inst Metals (1952) 80, p 577.

36. L. Pauling: Atomic Radii and Interatomic Distances in Metals. Jnl American Chemical Society (1947) 69, pp 542-553.

37. W. J. Wrazej: Lattice Spacing of Retained Austenite in Iron-Carbon Alloys. Nature (1949) 163, pp 212-213.

38. J. Mazur: Lattice Parameters of Martensite and of Austenite. Nature (1950) 166, p 828.

39. For example: E. T. Montgomery, T. S. Shevlin, H. M. Greenhouse, and H. W. Newkirk: Preliminary Microscopic Studies of Cermets at High Temperatures. WADC Technical Report 54-33, Ohio State University, April 1955, pp 27-31.

40. E. M. Trent and A. Carter: Sintered Titanium Carbide Alloys. Preprint for Powder Metallurgy Symposium of the Iron and Steel Institute, 1st-2nd December, 1954, Group IV, p 20.

SUGGESTIONS FOR FURTHER RESEARCH

The principal difficulty encountered in this investigation was in achieving equilibrium without introducing oxygen contamination. Future work in this system should be conducted with equipment which will maintain a high vacuum.

Arc casting did not produce alloys which were suitable for studying compositions containing large amounts of titanium carbide, and powder metallurgy methods should be used in this region of the system. One procedure, which was initiated but not completed, involved the infiltration, in high vacuum, of binary compositions into beta + delta or delta + carbon alloy powders, obtained from ingots arc melted with iodide titanium. The powders were to be placed in graphite crucibles which had been lined with titanium carbide, and binary compositions were to be allowed to melt on top. Anneals of several hundred hours just below the solidus were to follow, after which the lattice parameters and microstructures were to be examined, and chemical analyses were to be made. Noninfiltrated powder was to be included in every run, and compared with the original material, as a check for oxygen contamination. Since alloys of uniform composition could be obtained by such a method, a reliable determination of the solubility of nickel in titanium carbide, over a range of carbon contents, might be possible.

The γ solvus might best be checked by diffusion techniques. Nickel titanium binary compositions could be induction melted and given long homogenizing anneals, before being worked, annealed, and rolled into strips, 0.010 to 0.050 inches thick. After checking the homogeneity magnetically, and the absence of oxides metallographically, 2 gram portions of the strips would be selected. These samples would be packed in spectroscopic graphite powder, and annealed in hydrogen for 10 to 1000 hours at each of several temperatures before quenching. After etching off the surface layers, the total carbon content would be analyzed. The same technique could be carried out with titanium carbide powder, although longer anneals would be required, and analyses for titanium would also be needed.

In conjunction with the procedure outlined above, the variation of lattice parameter in the saturated gamma solid solution might be obtained exactly by annealing high purity nickel powder, mixed with graphite or carbide to prevent sintering, at the same temperatures and for the same times as the strips. A high vacuum treatment just before the quench would be necessary to remove the occluded hydrogen.

In addition to future work on the ternary, examination of the binder-carbide equilibria in the quaternaries, Ni-Cr-Ti-C and Ni-Mo-Ti-C might be profitable, since most

cermets made in these systems are not at equilibrium as-sintered, and phase changes may occur with time at the service temperatures.

BIOGRAPHICAL SKETCH

Edward Roy Stover was born in Washington, D. C. in April, 1929. He attended schools in Arlington, Virginia, graduating from the Washington-Lee High School in 1946. He entered the Massachusetts Institute of Technology, and obtained a Bachelor of Science degree in 1950 and a Master of Science degree in 1952. He is a junior member of the AIME, and a member of the American Society for Metals, Sigma Xi, the American Ordnance Association, and the National Speleological Society. He holds a commission in the United States Army Reserve. His hobbies are sailing, spelunking, and photography.

APPENDIX: EXPERIMENTAL DETAILS

A. ARC MELTING

Figure A-1 illustrates the apparatus used for melting the alloys in a purified helium atmosphere.

Helium, under a few centimeters positive pressure, was passed through a flowmeter (A), and a cold trap (B). It could then be passed through a stainless steel tube (C) containing titanium chips at about 850°C, and into a charcoal trap (D), which was placed in liquid nitrogen. This trap was also attached to the vacuum line. For activating the charcoal, the trap was heated by a removable furnace to 500°C under vacuum.

The purified gas could then be passed into an evacuated 12 liter flask (E) at a slow rate (usually 50 - 200 liters per hour). It was held in the flask under about 10 cm positive pressure, and the volume was almost sufficient to fill the evacuated melting chamber to 1 atmosphere pressure. The chamber could be filled with the gas held in the reservoir, together with that in the purifying train, within a few seconds, thus minimizing contamination due to leakage into the chamber. Tank helium could also be passed directly into the chamber for flushing.

A mercury bubbler-manometer (F) prevented the pressure in the chamber from rising too high during melting. This attachment was desirable when melting TiC, although most of the alloys were melted in a closed atmosphere, and the

FIGURE A-1: ARC MELTING APPARATUS

A. Flowmeter and manometer.

B. Cold trap (in dry ice or liquid nitrogen.)

C. Furnace containing titanium chips.

D. Activated charcoal trap (in liquid nitrogen.)

E. Helium reservoir.

F. Mercury bubbler-manometer.

G. Mercury manometer.

H. Cold trap in vacuum line.

I. Thermocouple vacuum gauge.

J. Dust trap.

K. Nickel-plated copper crucible.

L. Radiation shields.

M. Push-rod manipulator.

N. Water-cooled electrode.

O. Extension arm.

P. Sliding counterweight.

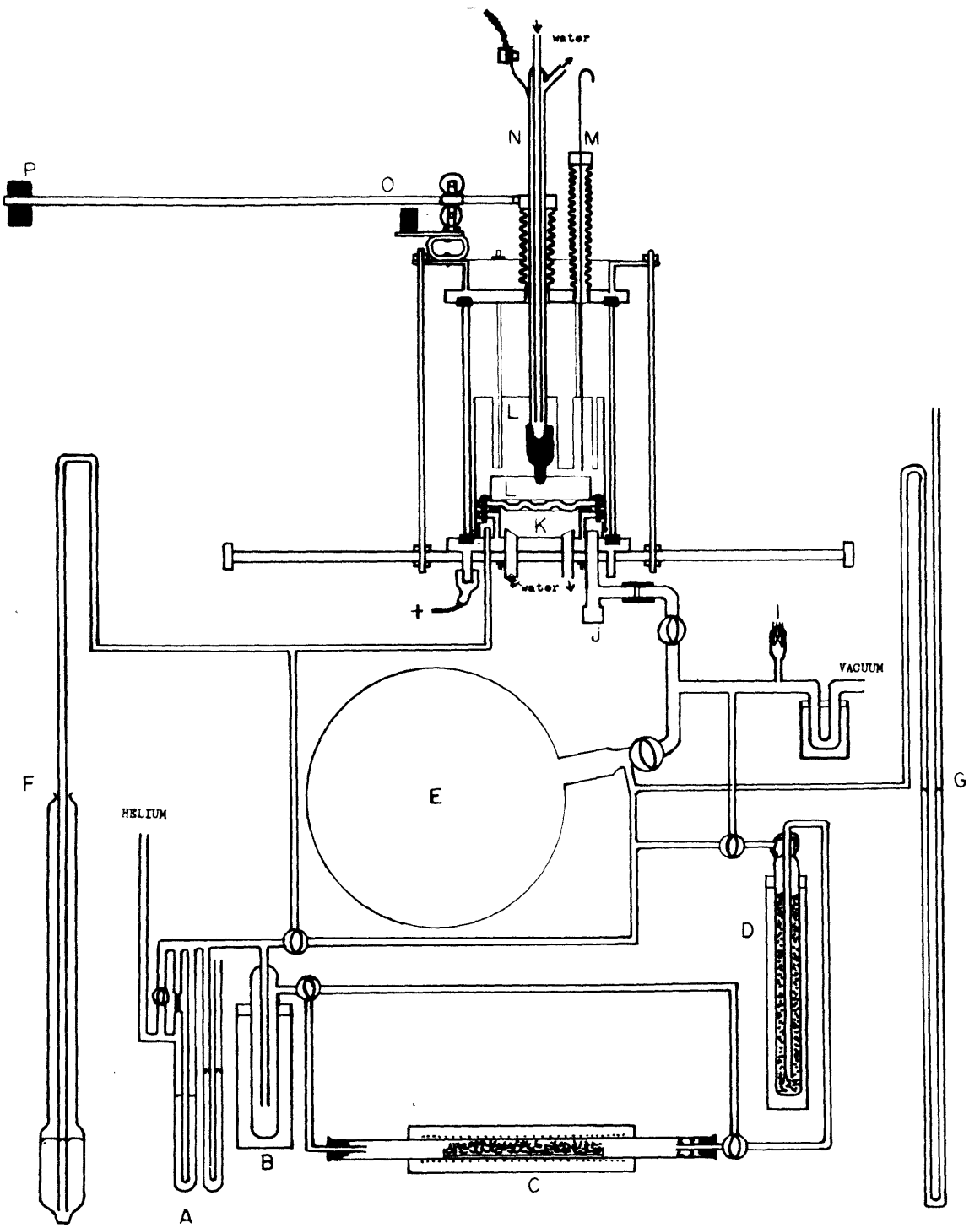
water
N
M
P
O
L
L
K
water
+
J
I
VACUUM
F
HELIUM
E
G
D
B
C
A

bubbler-manometer was replaced in these cases with a manometer similar to that attached to the reservoir.

The melting chamber itself consisted of a pyrex cylinder, 6 inches in diameter and 10 inches high, clamped between two neoprene gaskets mounted in brass plates. The crucible (K) was an indented 1/4 inch thick electrical copper plate, nickel plated on the top. It was clamped onto a silicone rubber gasket over the water chamber. Nickel or titanium radiation shields (L) protected the pyrex from the heat of the arc and spattered metal. The outer shield contained slits through which the melting was observed, and it was mounted on wheels, so the slits could be moved in front of clean portions of the glass at intervals during the melting.

A push-rod (M) was used for turning over the buttons and for rotating the outer shield. This rod, as well as the water-cooled electrode (N) were attached to the upper plate with soldered sylphon bellows. An extension arm on the electrode was free to slide in wheels attached to the upper plate; a counterbalance on the end was used to prevent the bellows from being strained when the chamber was evacuated.

The welding current was supplied by a Hobart direct current welder, connected to a 440 volt line, and was capable of delivering 300 amperes at 40 volts.

The usual procedure finally adopted for melting was as follows. Pieces of titanium, spectroscopic graphite, and one or two blocks of vacuum melted nickel were placed in

each large indentation in the plate. Titanium sponge was placed in other indentations. The chamber was closed and evacuated. Hot water, at 60°C, was run through the electrode, around the top plate, and under the crucible, until the vacuum dropped to about 15 microns. The chamber was then flushed rapidly with tank helium twice, and evacuated to a few millimeters of mercury. The chamber was immediately filled with purified gas from the reservoir and charcoal trap. (When the bubbler was used, the reservoir and trap were left connected to the chamber during melting.) The water temperature was then decreased to about 15°C, and the titanium sponge was melted. The charges were melted, and the buttons were turned over and remelted twice.

B. ANNEALING.

Figure B-1 illustrates the apparatus used for vacuum annealing the samples for magnetic analysis. A single-stage mercury diffusion pump, and a cold trap (in liquid nitrogen) produced a vacuum of 0.1 to 0.01 microns in the tube leading to the specimens. A McCloud type vacuum gage was connected to the system between the pump and the cold trap, or through a separate cold trap to the specimen tube.

The specimens were contained in a nickel sheet container, about 3/8 x 3/8 inches, which had radiation shields attached to the top and bottom. The container was held in a quartz or vycor tube, which was connected to a smaller vycor tube, which was in turn connected to the vacuum system through a graded seal.

The furnace consisted of a 3/4 inch zircon tube, wound with Kanthal A wire, imbedded in alundum cement. A gradient insulation helped compensate for convection currents, and pyrex wool plugs at the top and bottom also reduced the effects of such currents. The furnace slid vertically along three support rods, which could be moved slightly to position the furnace in line with the specimens. The furnace was heated by current from a Variac autotransformer, and a Foxborrow controller, operated by the platinum-rhodium thermocouple, bypassed a small resistance in series with the furnace. Temperatures up to 1300°C could be maintained within $\pm$ 5°C, provided the controller calibration was checked every few hours.

FIGURE B-1: APPARATUS FOR VACUUM ANNEALING

A. Cenco "Megavac" pump.

B. Thermocouple gauge.

C. Liquid air trap.

D. Mercury diffusion pump.

E. McCloud vacuum gauge.

F. Air pump.

G. Pyrex to vycor graded seal.

H. Furnace with gradient insulation.

I. Platinum - platinum plus 10 per cent rhodium thermocouple.

J. Cold junction.

K. Foxborrow temperature controller.

L. Quenching tank.

M. Mirror.

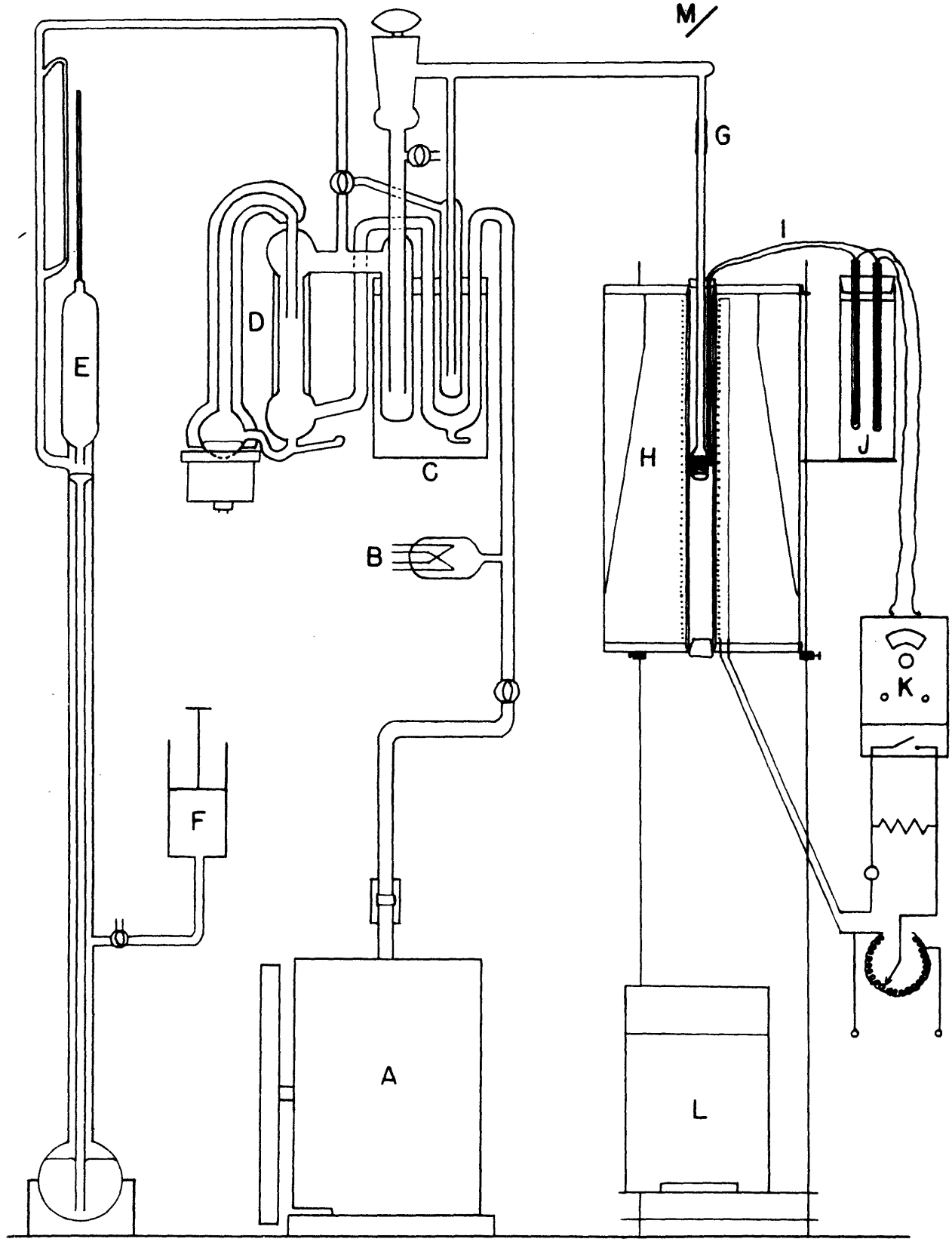
M
G
I
D
E
C
H
J
B
K
F
A
L

During a typical run, the samples were sealed in the tube, and the system was evacuated. The furnace was brought to temperature and raised to the proper position. The vacuum immediately dropped to a few microns as the specimens degassed, but five or ten minutes were sufficient for the vacuum to return to 0.1 micron. The temperature was checked periodically during the anneal with a Brown portable potentiometer. After the desired length of time, the vycor connecting tube above the furnace was either broken, or clamped and melted in two. The samples dropped into the quenching tank, and the bulb was instantly broken on the metal plate at the bottom.

Except when the vacuum was around 0.01 micron, a light oxide film or scale developed on the outside of the samples containing more than 2 atomic per cent titanium in solution. These samples were then heavily etched in a mixture of sulfuric and nitric acids, to which a little salt had been added, before they were reheated, or before the lattice parameters were determined.

C. MAGNETIC MEASUREMENTS.

Figure C-1 illustrates the apparatus used for measuring Curie points.

The assembly for holding the sample was divided into two parts. The lower half consisted of the furnace, made by winding glass insulated constantan thermocouple wire noninductively on a tube rolled from thin copper sheet. A piece of alundum thermocouple insulating tubing, 5/32 inch in diameter, was ground down at the upper end, and forced into the copper. The lower end of this tubing, which contained a copper-constantan thermocouple, was forced into a wooden block containing four brass screws. The lead wires for the furnace and thermocouple were soldered to copper or constantan springs, which were fastened to the block with the screws.

The upper half of the assembly contained a piece of oval alundum thermocouple tubing, about 1/16 x 3/32 inch, and 10 inches long. The two holes of this tube contained a thin nichrome wire, for support, and another thermocouple, which was lead out of the holes at the top of the tube down to two screws in the upper wooden block. The lower end of the alundum tube fitted into a quartz tube, about 5/32 inch O.D., which fitted snugly into the furnace. A brass strip, fashioned into a cup at the lower end, was inserted between the quartz and the alundum, and was crimped around the alundum just above the quartz. Another

FIGURE C-1: APPARATUS FOR MAGNETIC MEASUREMENTS

A. Specimen in brass cup.

B. Quartz tube.

C. Alundum two-holed insulation tubing.

D. Wooden blocks.

E. Jewelers' chain.

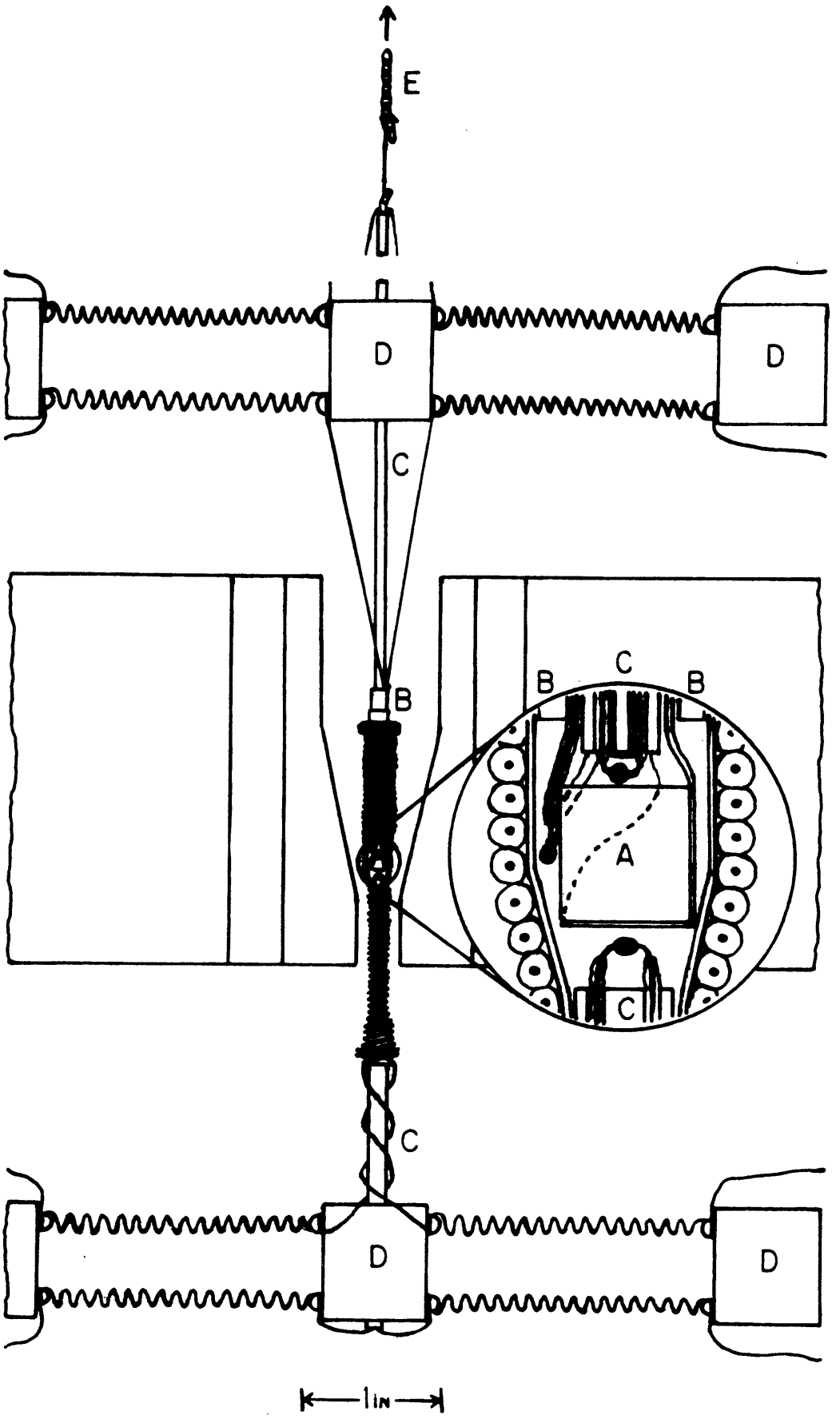
E
D
D
C
B
B
C
B
A
C
C
D
D
1 IN

thermocouple was also fitted between the quartz and alundum, and was placed at the side of the cup, which contained the specimen. The two halves of the assembly were wired together, so that all of the specimens were positioned in the same portion of the furnace, in the region of maximum temperature.

The entire assembly was supported by a copper hook, tied to the nichrome support wire. This hook fitted into a short length of jewelers' chain, with links 1/16 inch apart, so that the specimen could be moved through the magnetic field at intervals of 1/16 inch. The chain was attached to a balance mounted above the pole pieces. When all of the springs were compressed slightly, the entire assembly moved freely in a vertical plane, for balancing, but was not attracted to either pole.

The pole pieces were rectangular iron blocks, 1 inch wide and 2 inches long, milled to the shape illustrated in Figure C-1. The field between the poles was measured with a search coil, made by winding 26 turns of .0173 inch copper wire, in three layers, on a 0.0755 inch pyrex rod. The dimensions of the search coil were about 3/16 inch in diameter and 3/16 inch long. The current induced in the coil when the field was shut off was measured by the deflection of a ballistic galvanometer, calibrated with a known current sent through a mutual inductance of 50 millihenrys. The arrangement for these measurements is shown in Figure C-2.

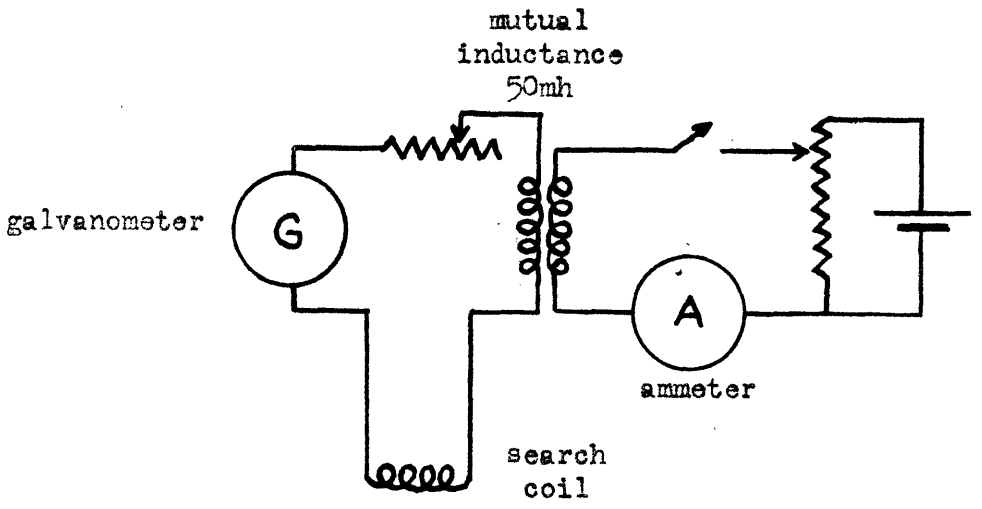

Figure C-2: Apparatus for field calibration.

The coil was calibrated in a known magnetic field of 1038 oersteds, which produced a current of 0.50 ma, using the arrangement illustrated. The field between the gradient pole pieces was obtained directly by comparing the deflection of the galvanometer with that obtained with a known current. The field gradient between the pole pieces, as a function of magnet current, is shown in Figure C-3. Figure C-4 shows the field in the region of maximum gradient over the range of fields used, along with the force on a nickel specimen in the same region, divided by its mass. The region of maximum force on the specimens was taken as the most accurate position of maximum field gradient, since the specimens were slightly smaller than the coil.

Due to the error in actual field gradient measurements, and slight differences in the weights and dimensions of the specimens, exact values of the magnetization, σ, versus temperature, were not obtained. However, since:

$$\sigma = \frac{F}{m} \cdot \frac{1}{(dH/dx)} ,$$

and all of the specimens were in the same position when measured, the force on each specimen, divided by the mass of the nickel in the specimen, was taken as proportional to σ at each field level. Samples of the same composition but of different weight were observed to have the same curves.

Measurements of F/m versus temperature were made on

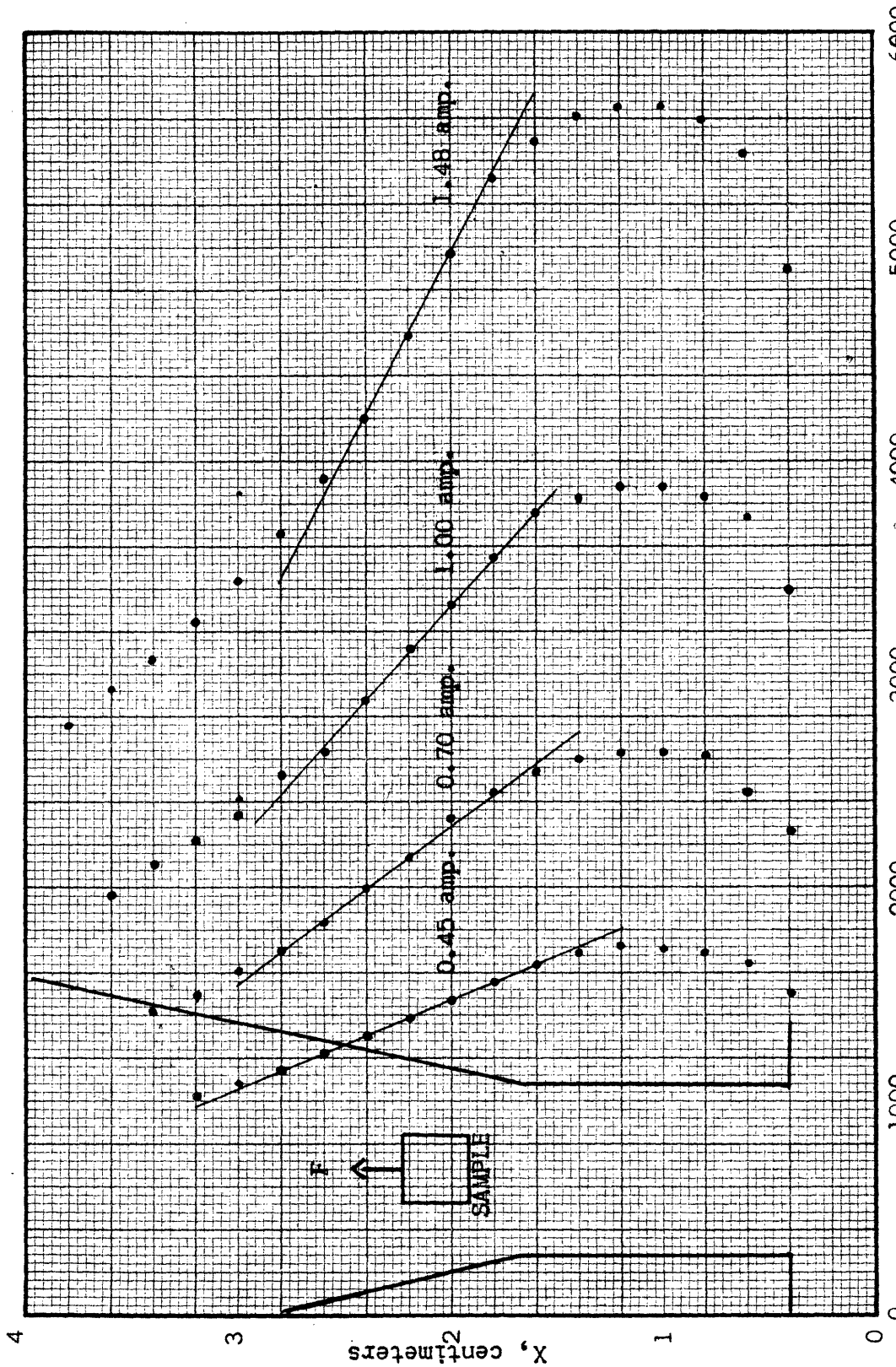

Figure C-3: Field gradient between poles at different magnet currents.

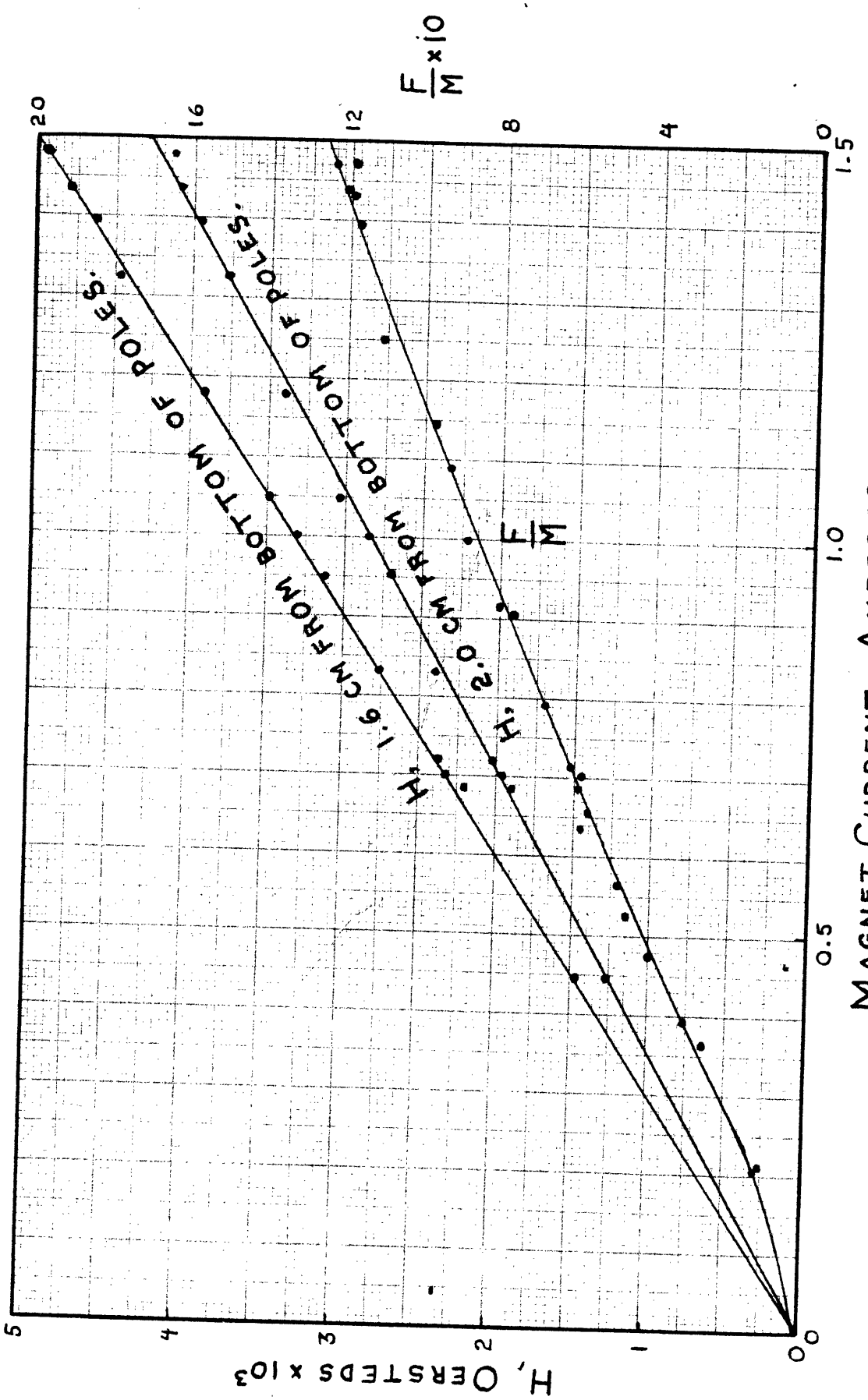

Figure C-4: Field as a function of magnet current.

both heating and cooling at two different magnet currents, 0.700 amperes, and 1.470 amperes, corresponding to 2100 and 4620 oersteds, respectively. Currents up to 7.5 amperes could have been used, but at the higher ranges, the curve of field versus current was no longer linear, and resistance heating in the magnet windings made it difficult to maintain a constant field. The values chosen were in a region in which the field was approximately proportional to the current, and allowed the use of one scale on the ammeter.

Figure C-5 shows the magnetization curves obtained for pure nickel. The curves made at the lower field were multiplied by a factor equal to the differences in forces at room temperature. Since the differences in σ due to differences in field become noticeable only near the Curie point, the differences in forces at a relatively low temperature should be equal to the differences in field gradients corresponding to the two fields. Thus, curves proportional to σ were obtained for the two fields, and these curves could be extrapolated by the Weiss method, as shown in Figure C-5. Briefly, this involves an extrapolation of the temperatures of different portions of the curves versus the field, to obtain a curve at zero field, and the extrapolation of the square of this curve to zero σ to obtain the temperature of the Curie point, by Weiss's definition. It was observed that by this method, slight differences in the multiplying factor, while shifting the

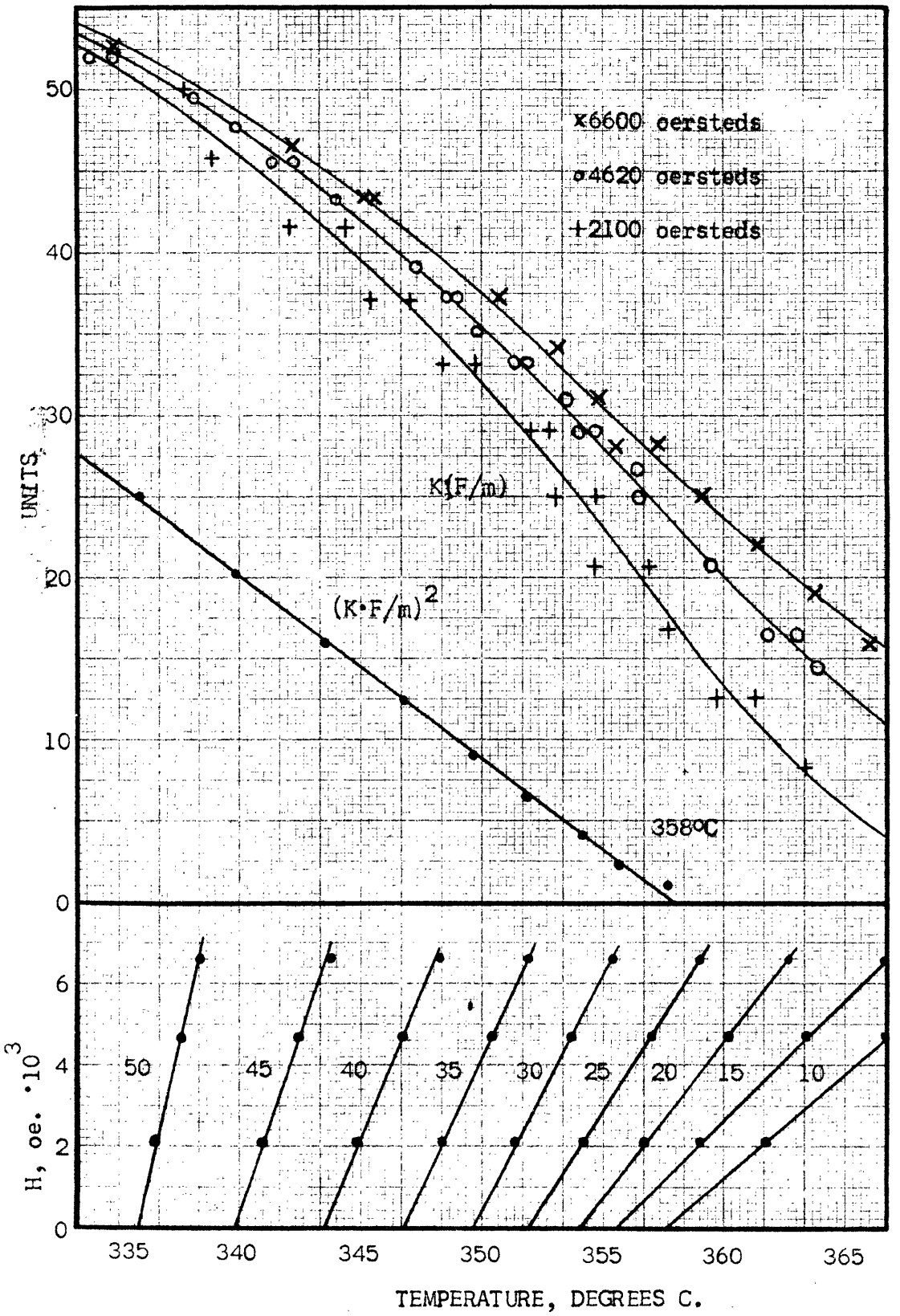

Figure C-5: Sample determination of the Curie point; pure nickel "B".

level of values on the curve of lower field, and hence the height and slope of the curve at zero field, did not change the extrapolated value of this curve at zero field.

It was observed that the slope of the magnetization versus temperature curves changed with the composition. Marian (reference 20) observed this same effect, which is usually blamed on alloy inhomogeneity. In Figure C-6, the slopes of all of the curves at 1.47 amperes are plotted against the Curie points. Some of the scatter is due to the uncertainty in exact sample composition, but those points showing the greatest deviation from the Ni - Ti binary alloys are those containing the greatest amount of carbon. This may be an indication of microsegregation of carbon in these samples.

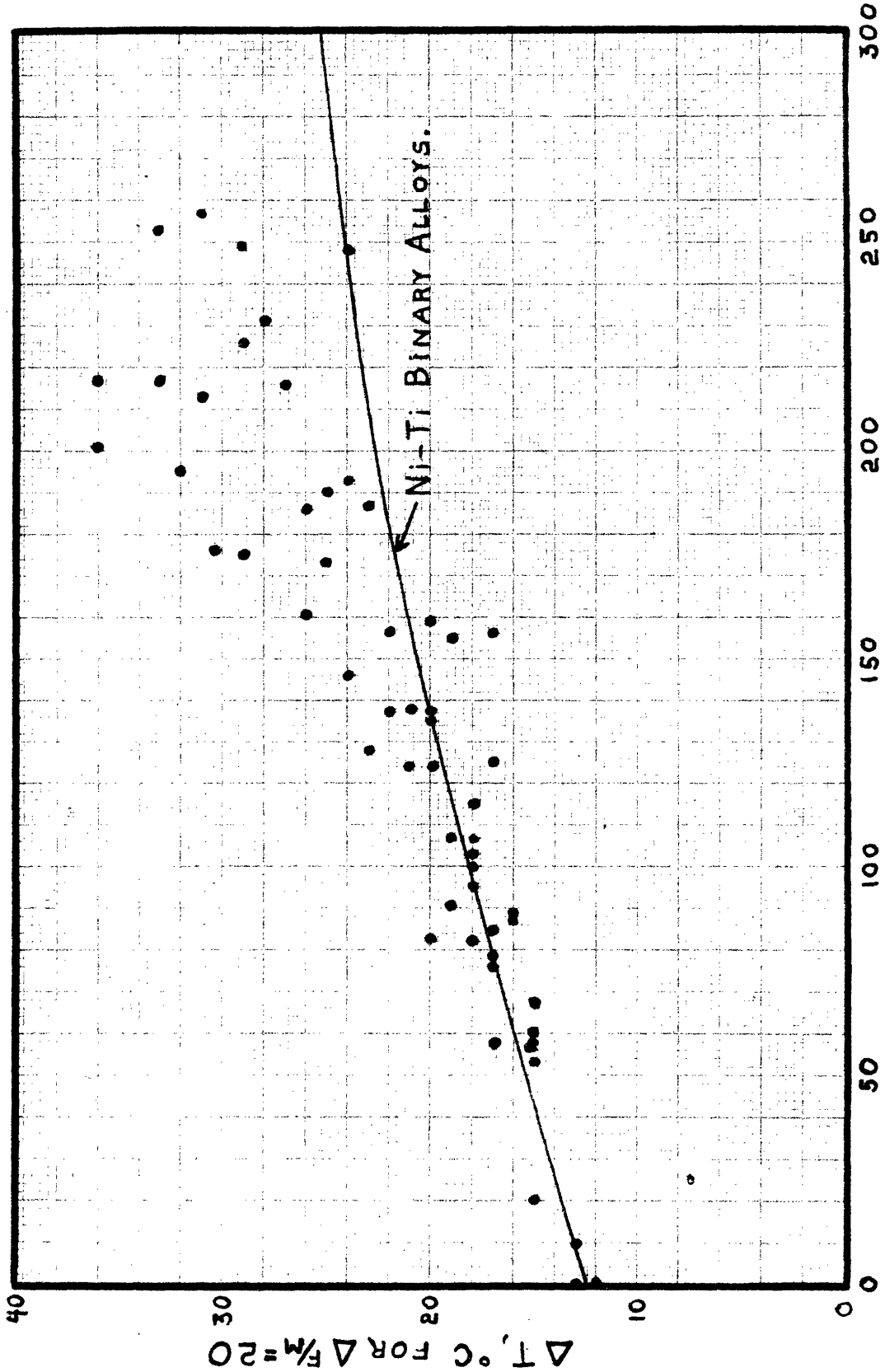

Figure C-6: Change in slope of K(F/m) vs. T curve with Curie point (or composition.)